POLYTECHNIC OF TURIN

MASTER's degree in AEROSPACE ENGINEERING

MASTER's Degree Thesis

Conceptual design methodology and tools for human Mars landers: Subsystems Design

Supervisors

Prof. Roberta FUSARO
Prof. Nicole VIOLA
Doc. Giuseppe Narducci

Candidate

Alessandro MAGLIO

JULY 2024

Abstract

The main goals of NASA's Evolvable Mars Campaign (EMC) include expanding the human presence on Mars by 2030 to promote scientific progress, innovation and international collaborations. This campaign, therefore, requires the development of new technologies to support the human presence and to transport heavy cargo to Mars. Thus, the development of multifunctional and reusable landers including the Mars Ascent Vehicle (MAV) is critical.
This thesis addresses the preliminary sizing of the major subsystems of a manned Mars lander with the ability to descend and ascend from Mars orbit. The goal is to deliver a tool requiring a limited set of users' inputs to select that will allow for a set of outputs calculated through specific algorithms. These inputs are design variables that are obtained from an initial phase of study and research on the state of the art of current technologies concerning Martian manned landers. Then these inputs will be used to obtain outputs that represent the preliminary sizing of the subsystems that will characterize the lander, which are: Attitude & Orbit Control System (AOCS), Environmental Control & Life Support System (ECLSS), Propulsion system, Thermal Protection System (TPS), Structure, Avionic System, Thermal Control System (TCS) and Electric Power System (EPS). The various sizing algorithms are designed to provide different outputs depending on the user's choice of different types of inputs. The main focus of the thesis will be on the sizing of the subsystems and validation of the results obtained, however, the first steps of the design will be analyzed through statistical analysis.
Detailed integration with the mission analysis part is left as future development with the goal of creating a valid methodology for lander design that can be implemented within a tool.

Table of Contents

Lyst of Figures ..... **V**

List of Tables ..... **VII**

Acronyms ..... **VIII**

1 Introduction **1**

1.1 Unmanned Mars Mission & Mars Lander **1**

1.2 Design of Manned Mars Mission **2**

1.3 Thesis Objectives & Breakdown of Work **4**

1.4 Research Outline **5**

2 Literature Review **7**

2.1 Launch Vehicle **7**

2.2 Mars Entry Descent & Landing **9**

2.2.1 Different reference architecture 9

2.2.2 Rigid Aeroshell 10

2.2.3 Hypersonic or Supersonic Inflatable Aerodynamic Decelerator (HIAD, SIAD) 11

2.2.4 All Propulsion Architecture 13

2.3 Mars Ascent Vehicle: generalities **13**

2.3.1 Orbits and stages 14

2.3.2 Structure 15

2.3.3 Propulsion System 17

2.3.4 Environmental & Control Life Support System 19

2.3.5 Thermal Control System 20

2.3.6 Thermal Protection System 22

2.3.7 Avionic System 22

2.3.8 Guidance Navigation & Control 23

2.3.9 Electrical Power System 23

3 Statistical Analysis **25**

3.1 Data collection in a database **25**

3.1.1 Mars Ascent Vehicle database 25

3.1.2 Mars Ascent Vehicle database graphs 29

3.1.3 Entry Descent Landing Database 31

3.1.4 Entry Descent Landing database graphs 32

3.2 First Design Methodology & Starting Point for Subsystem Design 34

4 Subsystem Design 36

4.1 Optimal Staging 36

4.2 Attitude & Orbit Control System 37
4.2.1 Inputs & Outputs 37
4.2.2 Sizing Algorithm 38

4.3 Environmental Control & Life Support System 41
4.3.1 Inputs & Outputs 42
4.3.2 Sizing Algorithm 42

4.4 Propulsion System 47
4.4.1 Inputs & Outputs 48
4.4.2 Sizing Algorithm 48

4.5 Structure 52
4.5.1 Inputs & Outputs 53
4.5.2 Sizing Algorithm 53

4.6 Thermal Protection System 54
4.6.1 Inputs & Outputs 55
4.6.2 Sizing Algorithm 56

4.7 Avionic System 59
4.7.1 Inputs & Outputs 60
4.7.2 Sizing Algorithm 60

4.8 Thermal Control System 61
4.8.1 Inputs & Outputs 62
4.8.2 Sizing Algorithm 63

4.9 Electrical Power System 66
4.9.1 Inputs & Outputs 67
4.9.2 Sizing Algorithm 68

4.10 New subsystems percentages on ascent dry mass 73

4.11 Architecture Change 74
4.11.1 Assumption 74
4.11.2 ADEPT 74
4.11.3 Capsule 76

5 Validation 78

5.1 Attitude & Orbit Control System 78

5.2 Enviromental Control & Life Support System 79

5.3 Propulsion System 80

5.4 Structure 81

5.5 Thermal Protection System 82
5.6 Thermal Control System 83
5.7 Electrical Power System 84
6 Conclusion and future works 86
6.1 Final results discussion 86
6.2 Improvements for future works 87
Bibliography 89

Lyst of Figures

Figure 1: Curiosity's 'Rocknest' Workplace 2
Figure 2: Mars Design Reference Architecture 5.0 mission sequence summary .. 4
Figure 3: Breakdown of Thesis Work 5
Figure 4: Starship and Super Heavy 7
Figure 5: Starship crew (left) and uncrewed (right) configuration 8
Figure 6: Starship payload volume (dimensions in m) 8
Figure 7: EDL-SA proposed architectures for exploration class missions 9
Figure 8: Dimension of blunt body (left) and slender body (right) 10
Figure 9: Payload mass comparison between the two body 11
Figure 10: IRVE-3 Flight Configuration 12
Figure 11: Mass savings as a function of IAD's diameter 13
Figure 12: Martian Orbit 14
Figure 13: Ascent ΔV results for varying initial thrust-to-weight ratio, arrival orbit, and number of stages [12]. 15
Figure 14: First and Second Stages of a type of MAV 16
Figure 15: Mars lander concept with MAV. 17
Figure 16: MMH distribution system 17
Figure 17: Propellant options [15] 18
Figure 18: Propellant liquid temperature range and Mars surface temperature range [11] 18
Figure 19: Scheme of Air Circulation 20
Figure 20: Scheme of heat pipe [15] 21
Figure 21: Absorpivities and emissivities of various materials [15] 22
Figure 22: Example of required power 23
Figure 23: Battery comparisons 24
Figure 24: MAV Statistical Trends: Payload Mass - Total Mass 29
Figure 25: MAV Statistical Trends: Payload Mass - Dry Mass 30
Figure 26: MAV Statistical Trends: Total Mass - Thrust 31
Figure 27: TPS + Deceleration System Mass - Total Mass 33
Figure 28: TPS + Deceleration System Mass - Dry Mass 33
Figure 29: Statistical analysis summary work & next steps 34
Figure 30: Geometrical configuration for engine assemblies with Number engine>1 49
Figure 31: Concepts for Thermal Protection System 54
Figure 32: HIAD architecture 55
Figure 33: Lander structure from oxydizer tanks side 57
Figure 34: Lander structure from fuel tanks side 57
Figure 35: Torus Radius in function of total number of tori 58

Figure 36: Typical requirements of Sources of Voice, Video and Data information [25] 61
Figure 37: Performance comparison from nuclear electric generation devices... 71
Figure 38: Mass vervus payload power level 72
Figure 39: ADEPT components, deployment system..... 75
Figure 40: ADEPT bottom and side with dimensions 75
Figure 41: Capsule bottom and side with dimensions 76
Figure 42: Heatshield and backshell TPS 77
Figure 43: Future Improvements: Design Tool 88

List of Tables

Table 1: LOX/LCH4 Mission Data Table (MAV) 27
Table 2: Other propellants and atypical Missions Data Table (MAV)..... 28
Table 3: Single Stage LOX/LCH4 Missions Data Table (MAV)..... 28
Table 4: Single Stage Other Propellants Missions Data Table (MAV)..... 29
Table 5: MAV Statistical Equations: Payload Mass - Total Mass 30
Table 6: MAV Statistical Equations: Payload Mass - Dry Mass..... 30
Table 7: MAV Statistical Equations: Total Mass – Thrust..... 31
Table 8: EDL Mass Distribution [7][18][20][21][22][23][24]..... 32
Table 9: EDL Statistical equation: Dry Mass/Total Mass – TPS & Dec. Sys Mass 33
Table 10: AOCS validation values 79
Table 11: ECLSS validation values..... 80
Table 12: Propulsion System validation values..... 81
Table 13: Structure validation values 82
Table 14: TPS validation values..... 82
Table 15: TCS validation values..... 83
Table 16: EPS validation values..... 85

Acronyms

ACS: Atmosphere Control & Supply.

ADEPT: Adaptable Deployable Entry Placement Technology.

AFRSI: Flexible Reusable Surface Insulation.

AOCS: Attitude & Orbit Control System.

ARS: Air Revitalization System.

C&DH: Command and Data Handling.

DAV: Descent Ascent Vehicle.

ECLSS: Environmental Control & Life Support System.

EDL-SA: Entry, Descent & Landing System Analysis.

EDL: Entry, Descent & Landing.

F-TPS: Flexible Thermal Protection System.

FDS: Fire Detection and Suppression.

HIAD: Hypersonic Inflatable Aerodynamic Decelerator.

HMO: High Mars Orbit.

IAD: Inflatable Aerodynamic Decelerator.

LEO: Low Earth Orbit.

LMO: Low Mars Orbit.

MAV: Mars Ascent Vehicle.

MOV: Mars Orbiting Vehicle.

MTOW: Maximum Take Off Weight.

MTV: Mars Transfer Vehicle.

NTR: Nuclear Thermal Rocket.

PCC: Protective Ceramic Coating.

SHAB: Surface Habitat.

SIAD: Inflatable Aerodynamic Decelerator.

SPTO: Single Phase To Orbit.

THC: Thermal and Humidity Control.

TPTO: Two Phase To Orbit.

TRL: Technology Readiness Level.

T/W0: initial thrust-to-weight ratio.

Chapter 1

Introduction

Man has always felt the need to push his limits and push into the unknown, first by reaching and landing on the Moon, and in recent decades by reaching and landing on Mars. The goal of all this is to satisfy the perennial curiosity that resides in the human nature, the desire to search for possible traces of past and/or present life forms and to succeed in colonizing an environment other than Earth's. For this through space exploration, as the years have progressed, it has provided and provides for increasingly challenging missions in terms of duration and engineering.
One of the challenges of landing on Mars, in addition to the design of the craft and propulsion system that will allow it to get to the red planet, is to design a manned lander that will allow it to land on the Martian surface and assist the astronauts for the duration of the mission.
As for the architecture of the mission, there is no right or wrong one, but it must be tailored to the goals that want to be achieved.

1.1 Unmanned Mars Mission & Mars Lander

From a historical perspective, looking at the missions that have been made to Mars, the totality are unmanned robotic missions.
Among the most important ones are:

- NASA's Viking 1, which was the first spacecraft that successfully landed on the Martian surface. Viking 1 consisted of an orbiter and a lander, which through taking high-resolution images were tasked with studying the Martian atmosphere and surface, respectively. Operational since July 1976, this mission was planned to last 90 days, but both orbiter and lander were operational for more than 4 years [1].
- NASA's Mars Pathfinder operational from July 1997 until September of that year, landed a lander and a robotic rover on the Martian surface, the first rover in history to land on the Martian surface. Both rover and lander carried instruments to make scientific observations and to provide technical data on the new technologies used. This mission used an innovative method to land on the Martian surface formed by

a parachute to slow the vehicle's descent through the atmosphere and a giant airbag to cushion the impact [2].

- Mars Science Laboratory (MSL), still operational as of August 2012. The Curiosity rover was landed on the Martian surface using a giant parachute to slow its descent through the Martian atmosphere, a jet-controlled descent vehicle, and a system called "cranes from the sky." The rover's mission is to investigate the past and present ability of Mars to support microbial life [3].
- Mars 2020, operational from February 2021. The Perseverance rover was landed on the Martian surface, which unlike Curiosity, despicted in Figure 1 has as its main purpose to search for signs of ancient life and to collect samples to bring back to Earth in the future. About 85 percent of Perseverance's hardware is based on that of Curiosity, whose descent strategy it also used [4].

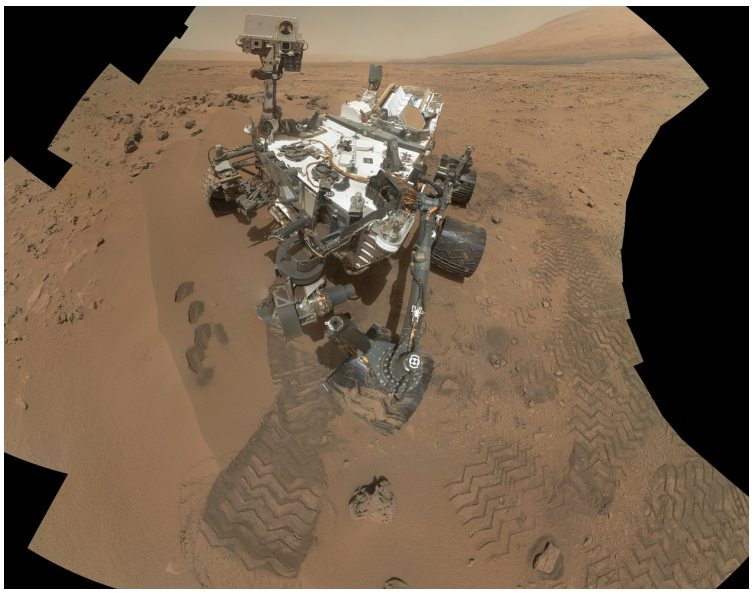

Figure 1: Curiosity's 'Rocknest' Workplace

In addition, these missions have also been used to try and test new technologies that can be implemented for hypothetical manned missions to the red planet.

1.2 Design of Manned Mars Mission

The main difficulty of a manned mission lies in the length of interstellar travel and the length of stay that one will have on Mars. This is because as the duration of the trip and mission increases, the resources to be carried

aboard the spacecraft and the exposure to cosmic radiation increase considerably. These 2 are the main problems to be addressed.
At present, no Mars manned missions have yet been performed or planned in the near term, but there are several papers that have tried to simulate hypothetical missions, one of which is a technical report from Nasa: "Human Exploration of Mars Design Reference Architecture 5.0, Mars Architecture Steering Group, 2009" [5].
This report describes three missions that would lead to human exploration of Mars. The number of missions was not chosen at random, this is because a single mission would have been too risky to send humans to Mars, while the 3 consecutive missions, to be done over 10 years, would have been safer. This is enough time to achieve the chosen goals and to develop new technologies and knowledge in the meantime to make future missions safer and more reliable for humans.
In addition, before the start of these three Mars missions, other test missions around the Earth, the Moon and Mars by robotic equipment are planned, so that more and more technologies can be tested and validated and human exploration on Mars can be made more feasible.
On each of these three missions, a crew of six is sent, each of whom will visit a different location on Mars. Each of the three missions will be "pre-deployed" or "split mission," that is, they will adopt a long-dwell trajectory; this means that a portion of each mission's assets are sent before the crew. This option fits well with the opportunity to use the Martian atmosphere as a source of raw materials to produce the ascent propellant in situ, to avoid transport of additional propellant resulting in a reduction in the size of the ascent lander.
The first phase of the mission architecture begins with the pre-deployment of the descent/ascent vehicle (DAV) and the surface habitat (SHAB). These two sets of vehicles are first launched, then assembled (via rendezvous and docking) and controlled in LEO. Once all systems have been verified and are operational, the craft depart at the opening of the Earth-Mars launch window, about two years before the crew launch. Interstellar travel will be accomplished using nuclear thermal rocket propulsion (NTR).
Upon arrival at Mars, the vehicles are taken into a high Martian orbit. The SHAB remains in Martian orbit in a semi-dormant mode, awaiting the arrival of the crew two years later. The DAV is captured in a temporary Martian orbit where it will enter, descend and land on the surface of Mars at the desired landing site. After landing, the vehicle is checked, the operability of its systems is verified, and then it is deployed. Later, the surface fission reactor is also deployed, so that production of the ascent propellant and other products needed by the crew can begin. A key feature of long-stay mission

architectures is the autonomous deployment of part of the surface infrastructure prior to the arrival of the crew.
The second phase of this architecture is characterized by the launch, assembly and checkout of the Mars crew transfer vehicle (MTV). The MTV serves as the crew's interplanetary support vehicle for a mission to Mars orbit and back to Earth. After all vehicles and systems, including the DAV (on the surface of Mars), SHAB (in Mars orbit) and MTV (in LEO) have been verified operational, the flight crew is placed on the fast transit trajectory to Mars. The duration of the transfer to Mars depends on the date of the mission and varies from 175 to 225 days. Upon arrival at Mars, crew members will rendezvous with the SHAB, which will serve as a transportation leg to the surface of Mars.

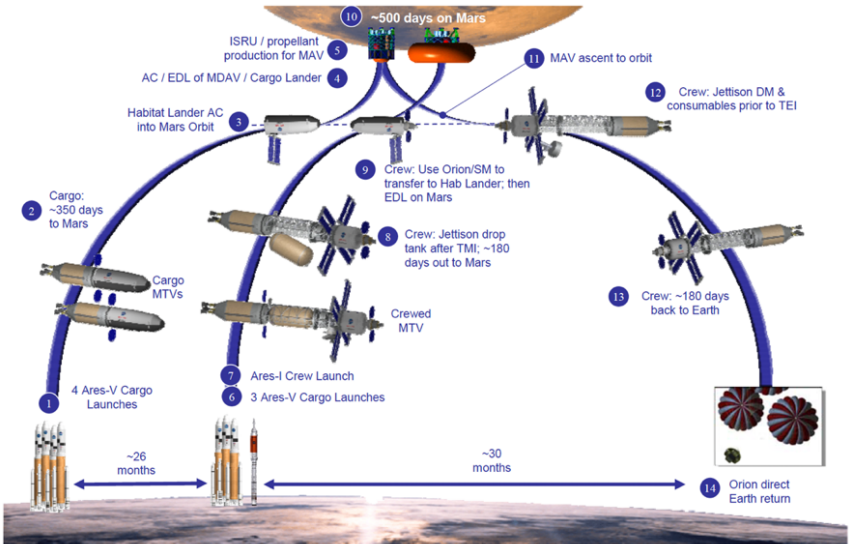

Figure 2: Mars Design Reference Architecture 5.0 mission sequence summary

After the crew has acclimated to Martian gravity, initial surface activities will focus on transitioning from a "lander mode" to a fully functional surface habitat.
The architecture of the long-stay mission lends itself to a very robust surface exploration strategy, in which the crew would have about 18 months to perform surface exploration as detailed in Figure 2.

1.3 Thesis Objectives & Breakdown of Work

The objective of the following thesis is to create a tool for the design of a manned Martian lander, focusing on the preliminary sizing of the various

subsystems that comprise it. Going into specifics, all the objectives of the thesis are:

1. Creation of a database containing information on MAVs, technologies used for EDL, and various types of simulated missions;
2. Creation of algorithms that allow for ad hoc sizing of the various subsystems of a manned Mars lander depending on the inputs that are chosen from time to time;
3. Validation of these algorithms.

This thesis work is conducted in parallel with a second thesis work that will instead focus entirely on the analysis and simulation of the ascent and descent phases of the mission. In Figure 3, the breakdown of the work into the various phases of the project is presented.

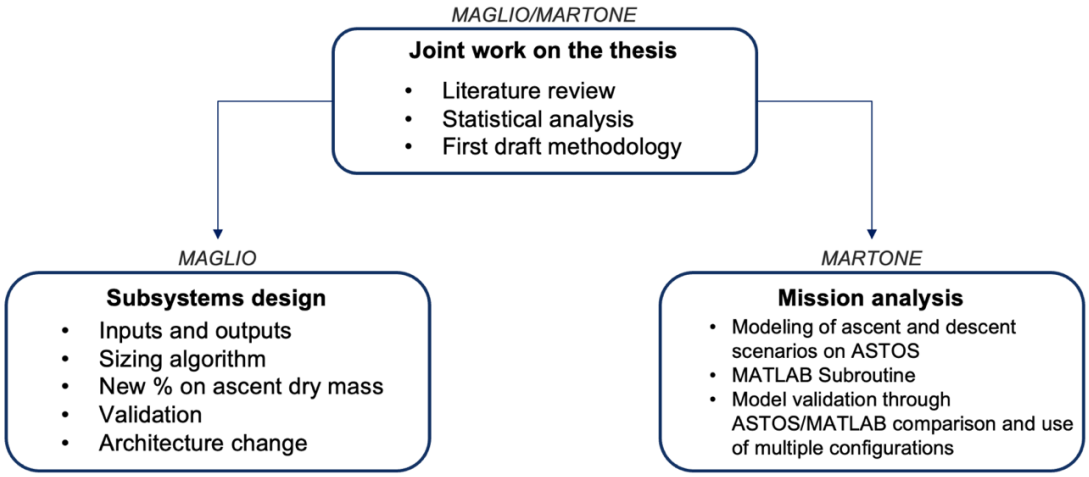

Figure 3: Breakdown of Thesis Work

1.4 Research Outline

The structure of the thesis is divided into several chapters.
Chapter 2 focuses on the literature review of all the papers that have served to give an overview of the state of the art of current technologies for Mars manned landers with a particular focus on the systems used to perform Entry, Descent & Landing (EDL) and the subsystems of which a Mars Ascent Vehicle (MAV) is composed.
In Chapter 3 a statistical analysis is done with much of the information gleaned from the literature review, with a particular focus on the various numerical data and mission types that will lead to the creation of graphs that will allow for a first draft methodology and inputs from which to start preliminary lander sizing.

In Chapter 4, methodologies for the design of each subsystem that characterizes a manned Mars lander are implemented, drawing up a list of inputs and outputs for each, and using ad hoc inputs to have a first estimate of the lander's mass, power, and volume budgets.
In Chapter 5, the various algorithms used to size the subsystems in the previous chapter are validated, carefully choosing inputs in of the other papers not used in the previous chapters.
Eventually, in Chapter 6, conclusions are drawn from the work done and some ideas for future studies will be proposed.

Chapter 2

Literature Review

This chapter will provide all the useful information about the different design options for manned Mars landers present in the current state of the art. There will be a special focus on the systems used for EDL and the various subsystems present on an MAV, with a list of their merits and drawbacks. All of this is useful for exploring the most advantageous configurations that can be considered in later chapters for lander design.

2.1 Launch Vehicle

Space X's Starship system was chosen to carry the lander into low Earth orbit (LEO). This transport system consists of two stages: the Super Heavy Rocket, which is the main booster, and the Starship, which represents the spacecraft. This system is fully reusable and is designed to carry out lander transport for future missions to the Moon and Mars. The system is depicted in Figure 4.

Figure 4: Starship and Super Heavy

Going into the details of the Starship depicted in Figure 5, it can carry different types of payloads including satellites, landers and rovers to any type of Earth orbit, lunar or Martian environments.
The fairing's standard fairing size is about 9 meters, and it represents the most commercially usable payload volume. The fairing remains closed throughout the launch until the payload is ready to be released [6]. The internal dimensions of the starship fairing are shown in Figure 6.

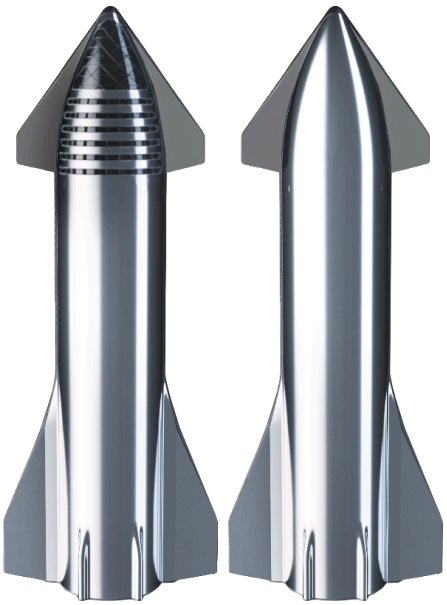

Figure 5: Starship crew (left) and uncrewed (right) configuration

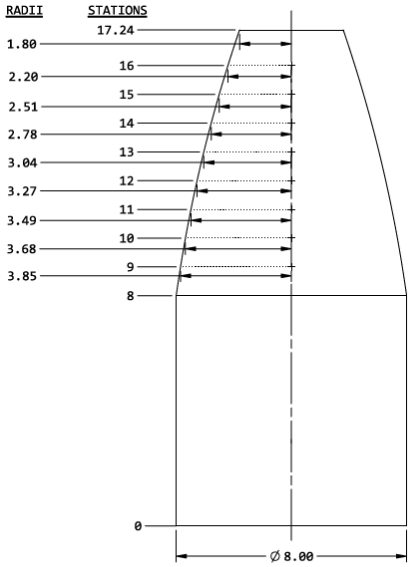

Figure 6: Starship payload volume (dimensions in m)

2.2 Mars Entry Descent & Landing

2.2.1 Different reference architecture

NASA, over the years, has been trying to develop high-fidelity models for Mars exploration missions regarding the simulation of the atmospheric entry, descent and landing phases, as there has been a shortage in this area.
To address this deficiency, a three-year activity called the Entry, Descent and Landing System Analysis (EDL-SA) was initiated, involving several research centers.
In this activity, an effort was made to identify technologies that could provide optimum performance in EDL. Specifically, the first year focused on missions where the landing payload is at least 40 tons, the second year there was a focus on carrying smaller payloads (1-3 tons, 3-5 tons), and the third year road maps were created for all mission classes. In [7] has as its main purpose to evaluate the technologies studied in the first year of the EDL-SA.
Figure 7 summarized of the various architectures studied and simulated.

	Aerocapture	Hypersonic	Supersonic	Subsonic
Architecture 1	Rigid Mid-L/D AS	Rigid Mid-L/D AS	Propulsion	Propulsion
Architecture 2	Lifting HIAD	Lifting HIAD	Propulsion	Propulsion
Architecture 3	N/A	Propulsion	Propulsion	Propulsion
Architecture 4	Rigid Mid-L/D AS	Lifting HIAD	Propulsion	Propulsion
Architecture 5	Rigid Mid-L/D AS	Lifting HIAD	Same LHIAD	Propulsion
Architecture 6	Lifting HIAD	Lifting HIAD	Same LHIAD	Propulsion
Architecture 7	Rigid Mid-L/D AS	Rigid Mid-L/D AS	Drag SIAD	Propulsion
Architecture 8	Lifting HIAD	Lifting HIAD	LSIAD–Skirt	Propulsion

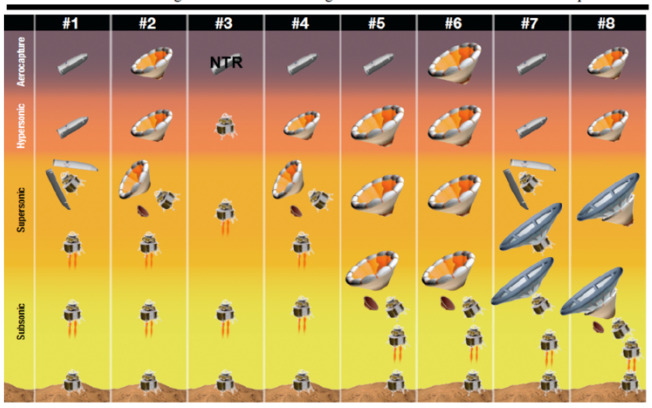

Figure 7: EDL-SA proposed architectures for exploration class missions

A total of 8 architectures have been proposed and simulated, some of which include the use of hypersonic and supersonic inflatable aerodynamic decelerators (HIAD and SIAD) combined with supersonic or subsonic retropropulsion technologies, others using a Mid L/D for the aerocapture and entry phase and supersonic retropulsion descent and landing phases, yet another using a fully propulsive solution instead.

All the mass, aerodynamic, and aerothermal models related to aerocapture, Thermal Protection System, and retropulsion were evaluated and simulated through the POST2 (Program to Optimize Simulated Trajectories) program that analyzes the various phases of the mission.
Some of the technologies used in the architectures of our interest will now be analyzed.

2.2.2 Rigid Aeroshell

Architecture 1 consists of a Mid L/D rigid aeroshell for aerocapture and hypersonic flight in the orbit entry phase, while supersonic retro-propulsion is used for the descent and landing phases.
This configuration has high technological maturity and reliability (high TRL) compared to the technologies used in other architectures, but is characterized by higher complexity in being modeled, packing, and separation during the various phases of the EDL.
In the scientific paper [8], special emphasis is placed on the shape of the vehicle entering the Martian atmosphere and two bodies are examined: a slender body with an L/D ratio of 0.68 similar to that of the previously named architecture 1 and a blunt body with an L/D of 0.3.

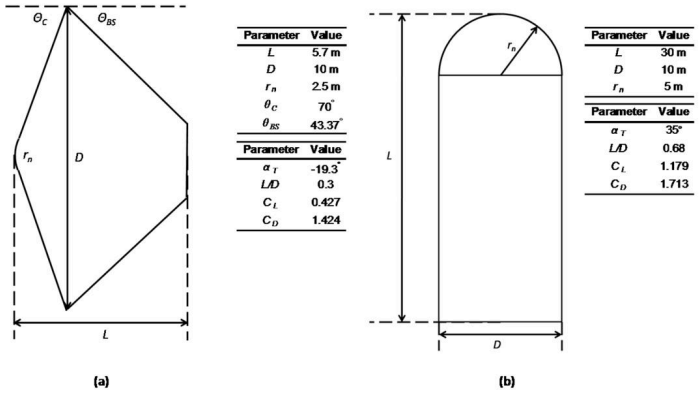

Parameter	Value
L	5.7 m
D	10 m
r_n	2.5 m
θ_C	70°
θ_{BS}	43.37°

Parameter	Value
α_T	-19.3°
L/D	0.3
C_L	0.427
C_D	1.424

Parameter	Value
L	30 m
D	10 m
r_n	5 m

Parameter	Value
α_T	35°
L/D	0.68
C_L	1.179
C_D	1.713

Figure 8: Dimension of blunt body (left) and slender body (right)

Slender bodies with a high L/D allow better handling in the maneuvers of the final stages of descent, while blunt bodies with a lower L/D are characterized by a smaller exposed surface area, thus a lower payload and consequently a lighter thermal protection system, resulting in savings on the total weight of the lander.
Comparing the two options shown in Figure 8, can be reasoned about the payload mass fraction: in Figure 9 can be seen that as the input mass increases, the gain we have in transportable payload decreases, resulting in a decrease in the payload mass fraction. Going into the specifics, there is an increase in transportable payload weight, but the increase in payload is less

than the increase in the initial mass of the whole system, and hence the decrease in payload mass fraction is justified.

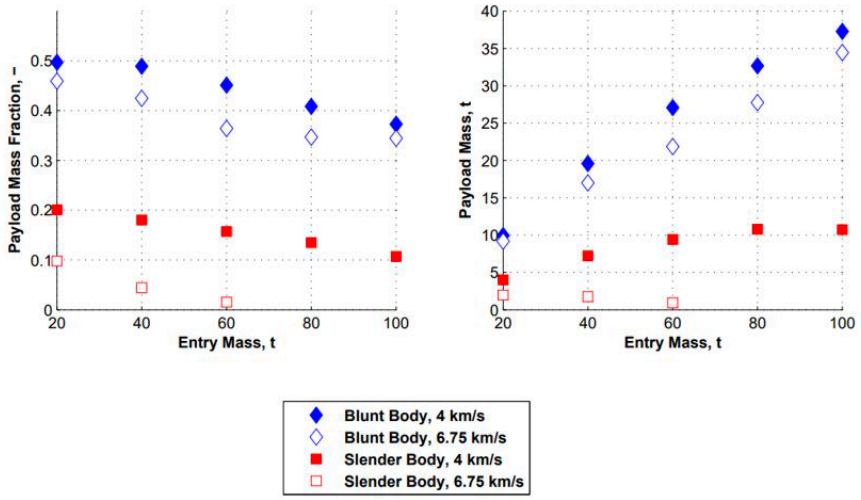

Figure 9: Payload mass comparison between the two body

Reasoning instead about velocities, using a direct entry inside the Martian atmosphere with a velocity of 6.75 km/s results in a reduction of the payload mass fraction by 15 percent compared to an entry with an orbital velocity of 4 km/s.

2.2.3 Hypersonic or Supersonic Inflatable Aerodynamic Decelerator (HIAD, SIAD)

The IAD (inflatable aerodynamic decelerator) is a type of flexible thermal protection system (F-TPS) that consists of a deployable aeroshell consisting of an inflatable structure that maintains its shape during atmospheric flight. If the aeroshell is deployed at the time when the vehicle's descent speed is hypersonic it is called HIAD, if the speed is supersonic then it is called SIAD. This type of technology is built in such a way as to increase drag during the descent phase within the atmosphere and functions as a primary heat shield. As for human Mars missions, this technology is being preferred for the descent phase of the EDL, this is because the Mars atmosphere is too thin compared to that of Earth to provide adequate deceleration, but it is dense enough to generate heat and ruin the lander's surface.
This IAD is lighter than the rigid aeroshells because of the lighter and more flexible materials from which it is composed, and so in the case where it is necessary to land a huge payload weight on the Martian surface and reducing the ballistic coefficient and heat spike at the same time, it is preferable to use the deployable flexible aeroshell.

The design of these structures is based on the construction of stacked toroids, in which there are a different set of tori that increase the resistant area and serve as structural support for the protective thermal layers. Usually, a nitrogen tank is used to pressurize the tori in the aeroshell [9] while as for the choice of stacked toroid configuration it comes from a series of experiments conducted on IADs that were deployed during descent through the Earth's atmosphere (IRVE 1, 2, 3). The third experiment, as shown in Figure 10, involved 7 toroids consisting of Kevlar tubes held together by radial straps in such a way as to minimize oscillations [10].

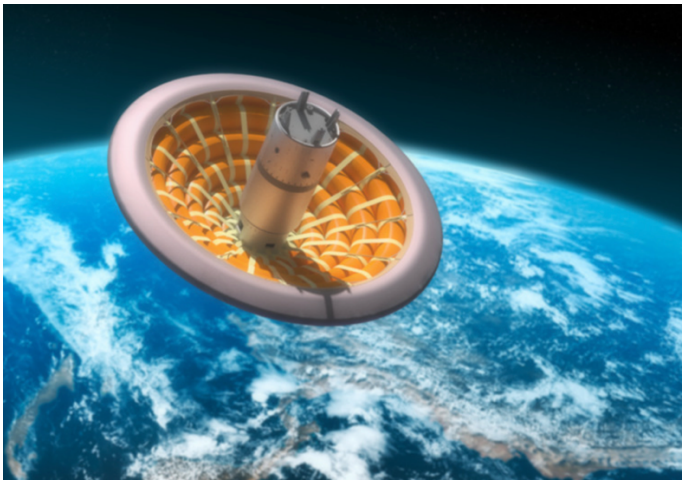

Figure 10: IRVE-3 Flight Configuration

Returning to the architectures of the EDL-SA [7], architecture 2 uses a 23-meter diameter HIAD for aerocapture and entry phase, while using supersonic back-propulsion for the descent and landing phase. With this configuration there is a 25-ton savings over the first architecture, but it uses technology with a lower TRL. Architecture 4, on the other hand, uses a rigid aeroshell for the aerocapture and a HIAD for the entry phase, allowing more entry mass to be carried on the surface due to the 4-ton lighter HIAD. Then supersonic and then subsonic propulsion are used for the descent and landing phase. The utilization of two different systems for aerocapture and entry increases the complexity of the whole system, and this makes the architecture less feasible to implement. Architecture 5, unlike Architecture 4 uses one HIAD with a larger diameter (68 meters) ejected once it reaches a subsonic velocity, and then uses subsonic retro-propulsion for final descent and landing. Architecture 6 uses a single 82-meter HIAD for aerocapture, entry, and for descent to subsonic velocity, and then uses subsonic retro-propulsion. The problem with the last 2 architectures described is that the mass model for such large HIADs is not very reliable.

2.2.4 All Propulsion Architecture

Architecture 3 proposes an all-propulsion solution, and it is the architecture with the highest TRL and the lowest complexity, since only engines are used, thus of existing and already used technologies. However, there is the problem of the interaction between the structure and the engines in hypersonic and supersonic ranges, and there is not enough information about flow separation, vehicle control dynamics, drag, and aerodynamics, all of which bring unknowns about thermal stress.
In addition, another problem concerns the masses on arrival, as this architecture has much higher masses on arrival than the others, also due to the huge amount of propellant that must be carried and used.
In [8], the important issue of choosing the diameter of the IAD is also addressed. Indeed, in Figure 11, supersonic retro-propulsion is useful for carrying only small payload masses, while in general as the entry mass increases there is a need for an IAD characterized by considerable increase in diameter in order for it to carry an acceptable payload.

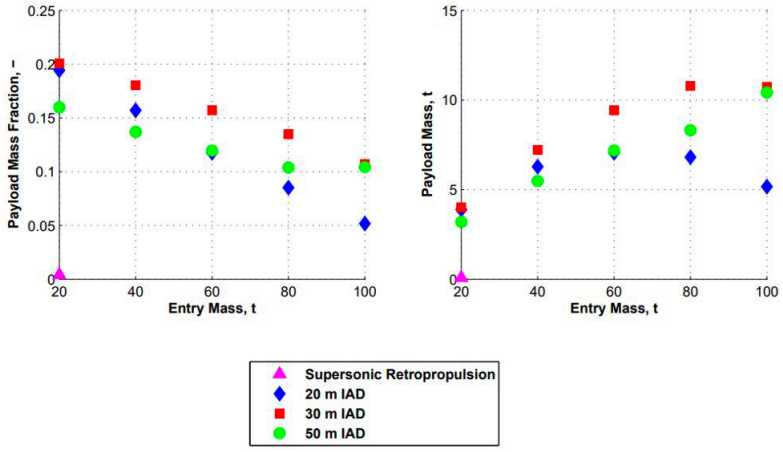

Figure 11: Mass savings as a function of IAD's diameter

2.3 Mars Ascent Vehicle: generalities

Focusing on the ascent phase, we will now discuss the MAV (Mars Ascent Vehicle), which is the vehicle that will be used by the crew to make the ascent from the Martian soil. This section will explain the various orbits that can be reached, the number of states from which it can be composed, and the state of the art of all the subsystems that make up this type of vehicle.

2.3.1 Orbits and stages

The orbits reached by the MAV during ascent are of different types and change depending on how the mission is set up. These orbits are called parking orbits, and they are reached by the MAV in such a way as to rendezvous with the vehicle that has been there for the duration of the stay on Martian soil and will allow the crew to return to Earth [11].
Specifically, in a study conducted by NASA [12], the number of TPTO (Two Phase To Orbit) and SPTO (Single Phase To Orbit) stages are analyzed and 3 ignitions are considered to reach the final parking orbit.
If the vehicle starts from a 100 x 250 km orbit, the main parking orbits considered are:

- Low Mars Orbit (LMO) (100 x 250km ⇒ 250 x 500km ⇒ 500km circular).
- High Mars Orbit (HMO) (100 x 250km ⇒ 250 x 250km ⇒ 250 x 33,793km).

The second orbit corresponds to the 1 Sol (1 Mars Day) orbit period.

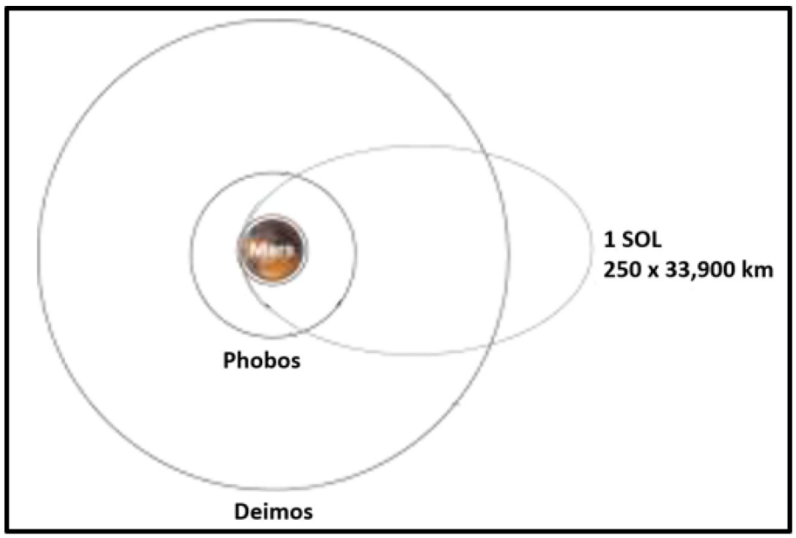

Figure 12: Martian Orbit

Figure 13 shows that considering the case study with LOX/LCH4 as the propellant, choosing either an LMO or HMO orbit, the two-stage option is always less heavy than the one-stage option, and this is due in part to the efficiency gained by staging.

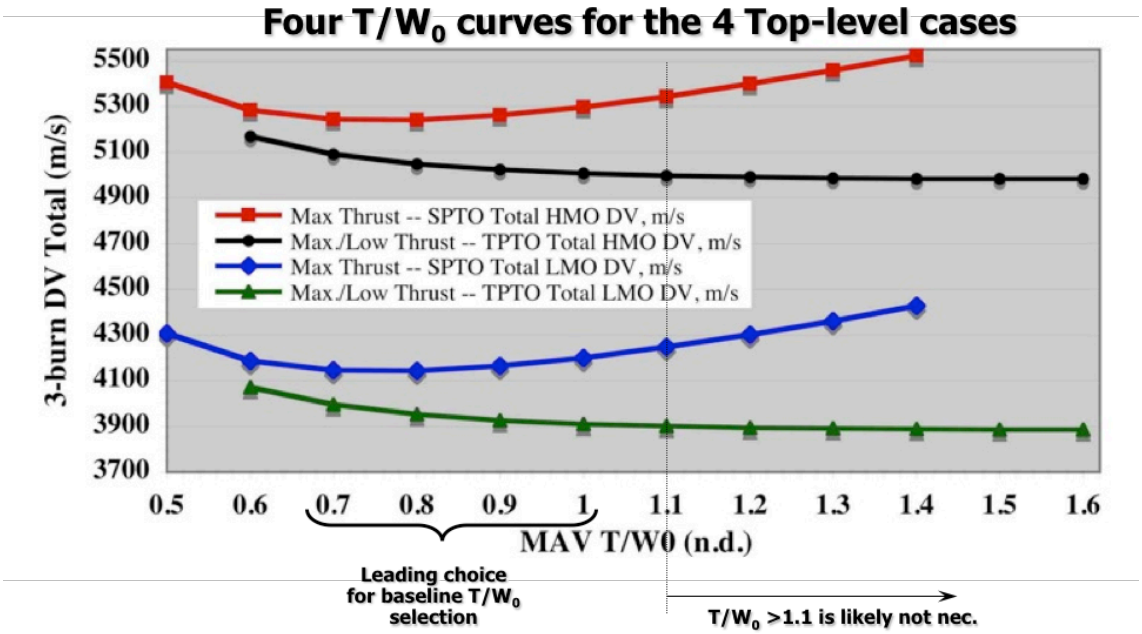

Figure 13: Ascent ΔV results for varying initial thrust-to-weight ratio, arrival orbit, and number of stages [12].

In addition, the thrust can vary greatly as T/W0 (initial thrust-to-weight ratio) changes, and that beyond a threshold value of this term, the gravity losses due to the trajectory that the MAV must follow to reach the parking orbit are no longer reduced. It is therefore good to keep the T/W0 ratio between 0.7-1. Additional problems that might arise if the Thrust is too high are that the mass of the propulsion system might grow too much, and too high accelerations might occur for the astronauts.

2.3.2 Structure

Usually, MAVs used in simulated manned missions have a very similar structure, characterized by a pressurized cylinder (pressurized capsule volume) that contains a livable space for the crew, a space for all equipment, and a space for all avionics and general electronic equipment.
This space varies depending on the amount of time the crew must spend on the Martian surface and inside the lander. Externally, around the cylinder diameter, there are usually tanks (usually spherical or cylindrical) for the propulsion system, while below the cabin are the engines and landing gear to allow stabilization on Martian soil and to support weight during landing. The landing gear legs are designed not to fail structurally in the unrated condition [13]. Usually, The MAV main structure frame is made of aluminum alloy [14].

The main capsule structure is reinforced with spars and ribs to withstand the non-pressure loads, i.e., those occurring during docking and dynamic loads during ascent [15].
In addition, the structure, if it consists of at least two stages, may lose components, such as engines or empty tanks, during ascent.

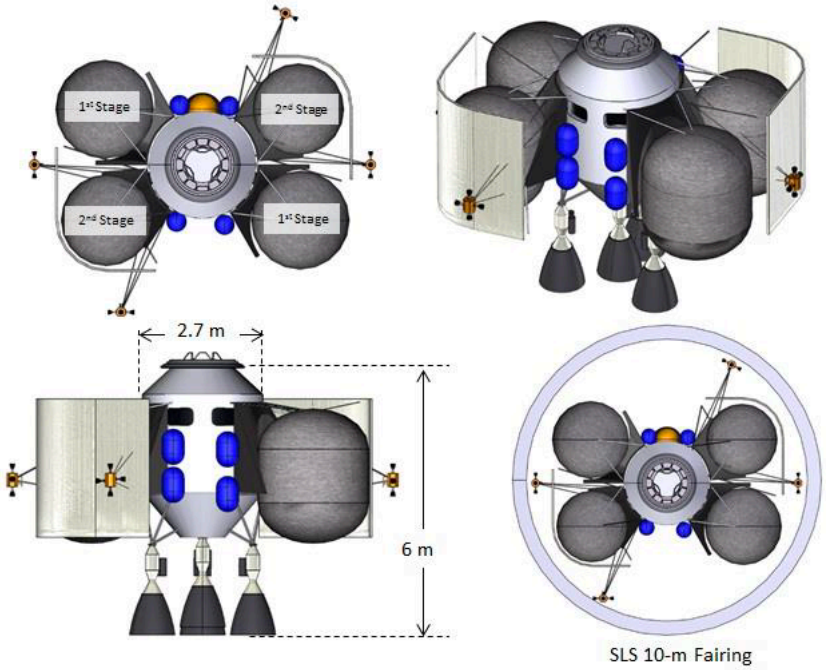

Figure 14: First and Second Stages of a type of MAV

Another concept structure for the MAV is those in Figure 15: Mars lander concept with MAV., with a cone shape that includes a hinges nose cone, which protects the docking ring and crew cabin access hatch during all phases of the mission. The MAV in question functions like that of the Apollo lander, as well as the crew exit and entry without an airlock is also like that of the lunar lander [16].

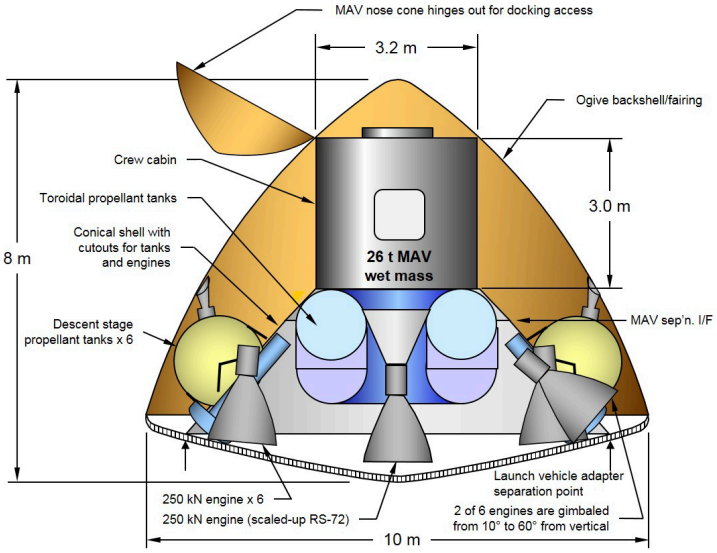

Figure 15: Mars lander concept with MAV.

2.3.3 Propulsion System

The propulsion system has the fundamental task of providing the MAV with the thrust it needs to make the ascent and to arrive at its intended parking orbit. It is one of the lander's heaviest systems because, excluding the propellant, it includes the mass of the tanks to hold the propellant an pressurizer, the weight of the engines themselves, and the weight of the entire propellant distribution system (feed system).

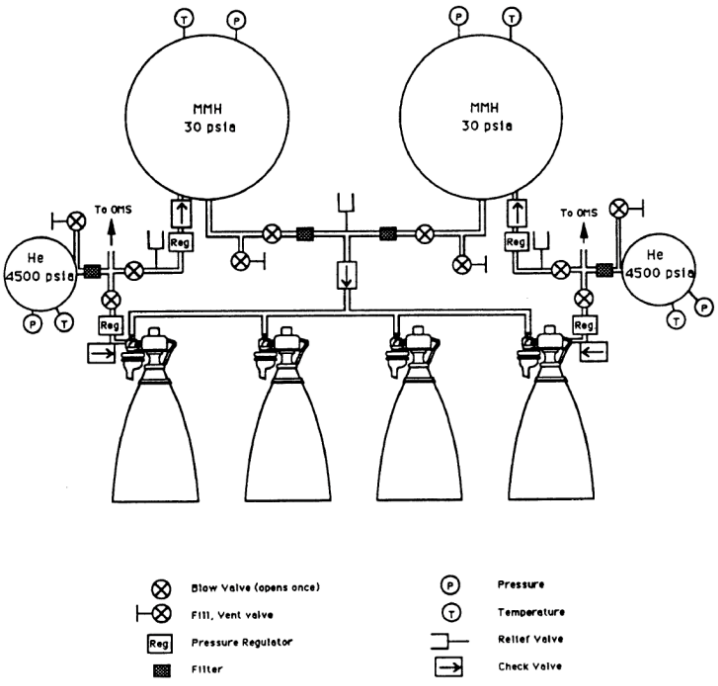

Figure 16: MMH distribution system

Regarding the propellants that can be used by the MAV, Figure 17 shows the main ones, associating the nominal specific impulse and mixture ratio with each.

Fuel	Oxidizer	Mass ratio (O:F)	Nominal I_{sp} (sec)
LH_2	LOX	6:1	460
Nuclear (LH_2)	--	--	850
MMH	LOX	1.4 to 1.6:1	380
MMH	H_2O_2	4:1	340
MMH, pumped	NTO	2:1	340
MMH, pressure-fed	NTO	1.6:1	320
Aerozine-50	NTO	2:1	310
N_2H_4 monoprop.	--	--	220
RP-1	LOX	2.6:1	330
Cold gas (N_2)	--	--	80
CH_4	LOX	3 to 4:1	380
C_3H_8	LOX	3.2:1	380

Figure 17: Propellant options [15]

Solid propellants have a specific impulse of between 200 and 300 seconds, which is less than that of liquid propellants, and therefore there will be a consequent increase in the total mass of the lander; they also do not allow for thrust adjustment, since once the spark is ignited the grain burns until it is exhausted [15].
In [11], there is a study in which various types of propellant and their physical state are analyzed depending on the equatorial temperature of Mars, which can range from 25 degrees Celsius to -70 degrees Celsius. In Situ Resource Utilization (ISRU) configurations using cryogenic propellants can be subject to boiloff, which makes the propulsion system more difficult to build and operate, requiring a cryocooler to keep the propellant in a liquid state. Figure 18 shows the range of Martian temperatures and gives a clearer picture of the ranges in which propellants are liquid.

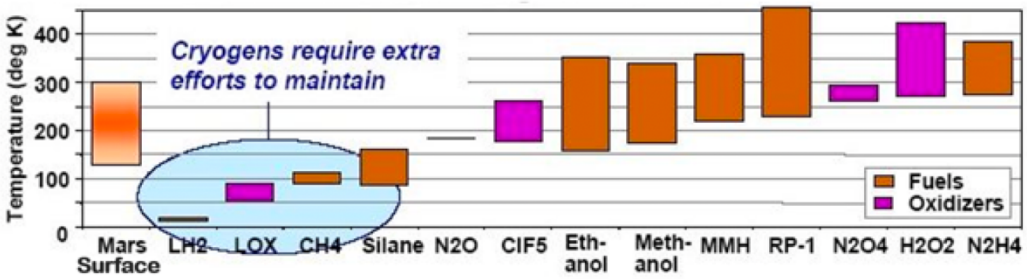

Figure 18: Propellant liquid temperature range and Mars surface temperature range [11]

One advantage of using ISRU configurations is the use of nontoxic propellants such as LO2 and LCH4. The disadvantage is that there is a need to use complex machinery to extract oxygen from the Martian atmosphere, which is 95% is composed of CO2.
The propellant feed system can be pressure feed or pump feed. The former has worse performance but higher reliability, as opposed to the latter, which has lower reliability but provides higher performance.
To be as conservative as possible, the propulsion system is sized so that the thrust generated by the motors is greater than the maximum thrust required during ascent [19].

2.3.4 Environmental & Control Life Support System

The task of the ECLSS is to provide an environment with all the necessary characteristics for the crew to enjoy good health under both nominal and nonnominal conditions.
The main tasks of the ECLSS are to maintain temperature, humidity, and pressure in predetermined ranges and to provide air, water, and food for the astronauts throughout their ascent and stay inside the MAV.
Usually, the atmosphere that is used inside the cabin enclosing the habitable volume is a mixture of nitrogen and oxygen. One could also opt for an atmosphere characterized by 100 percent oxygen, but the advantage of a simpler air distribution system is deterred by a higher probability of fire development and spread, so one usually opts for the safer alternative.
There is a system of fans and ducts throughout the cabin that circulates air, which is continuously supplemented with oxygen and nitrogen that are stored within special tanks. In case of failure of the air circulation system, there are vent valves on the nitrogen and oxygen tanks that allow manual release.
Also important is the air purification system, which allows contaminants and accumulated CO2 to be removed through a reaction with LiOH lithium hydroxide located in a bed.
To maintain the required humidity level within the cabin, there are water separators, which condense the water present within the atmosphere when necessary. To control temperature, thermistors are present, and to measure pressure, pressure transducers are present, which when needed activate pressure regulators that release or absorb oxygen.

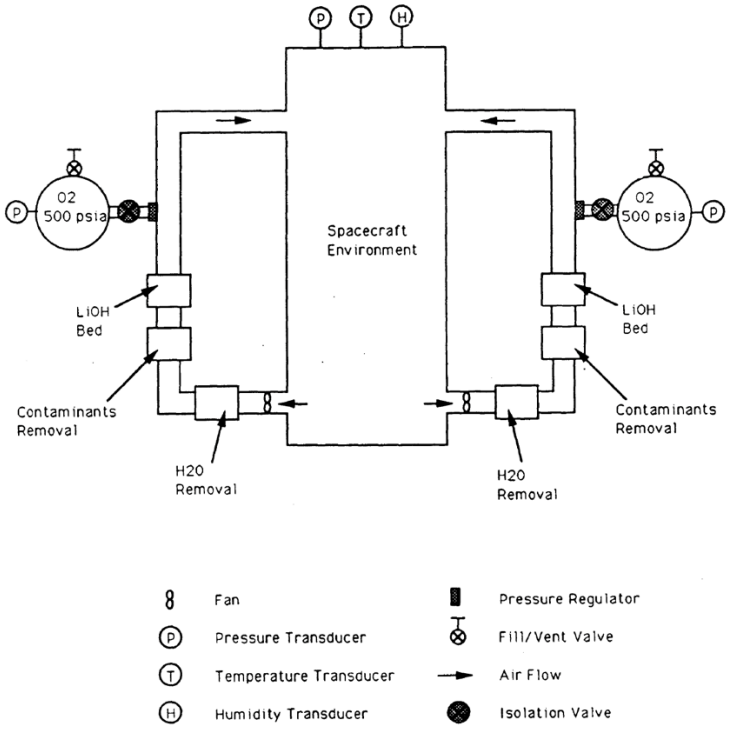

Figure 19: Scheme of Air Circulation

As for waste storage and management, it is not an important practice in case the MAV is used only for ascent, which has a limited time duration [15]. Finally, if the duration of the crew's stay inside the MAV does not exceed 30 days, there is no need for a radiation shield [13].

2.3.5 Thermal Control System

The Thermal Control System is a critically important subsystem for the MAV and performs three main functions:

1. Mitigating and limiting heat exchange between the aircraft and the multitude of external environments in which the MAV is expected to stop or pass;
2. Ensuring the proper temperature range for the components of the various subsystems or the atmosphere present within the MAV's pressurized volume;
3. Ensuring the right temperature range to the various propellants and pressurizers, this is because in an emergency, in order to perform an abort to orbit, the propellant must necessarily be liquid.

As mentioned earlier, the MAV must deal with different types of environments, including the Martian surface, the Martian atmosphere during ascent, and the vacuum of space at the time of rendezvous and docking with the MOV in the parking orbit [17].

These functions are performed using a few components: thermal coatings, heat transfer systems, and insulation systems.
Regarding insulation systems, there are two options: bulk insulation and vacuum system, and of the two, the former is the one is the easiest to implement. Regarding bulk insulation, foam insulation is the easiest to apply since it is applied directly to the surface of the lander and is the lightest and most self-supporting. While in terms of thermal conductivity, polyurethane insulation is the best. The alternative to bulk insulation are low-pressure insulation systems or vacuum systems. They are made by obtaining vacuum or at most low pressures in special compartments, to minimize thermal conductivity. Unlike bulk insulation, it is a more complex system to implement and there could be reliability problems as the vacuum creation system could fail.
As for heat transfer systems, there are many, and the two main options for collecting internally generated heat are: heat pipes and coolant loops. Coolant loops are cooling systems that use a cooling fluid (water or the propellant on the vehicle) that flows in pipes throughout the vehicle until the accumulated heat is rejected back into space through a radiator. The problem with coolant loops is the heaviness of the system. The heat pipe, on the other hand, is a closed tube that contains a working fluid and through porous capillary tubes that harness the latent heat of vaporization of the working fluid and subsequently transfer the heat from the area of interest to the radiator located on the outer surface of the MAV [15]. A scheme of heat pipe is rapresented in Figure 20.

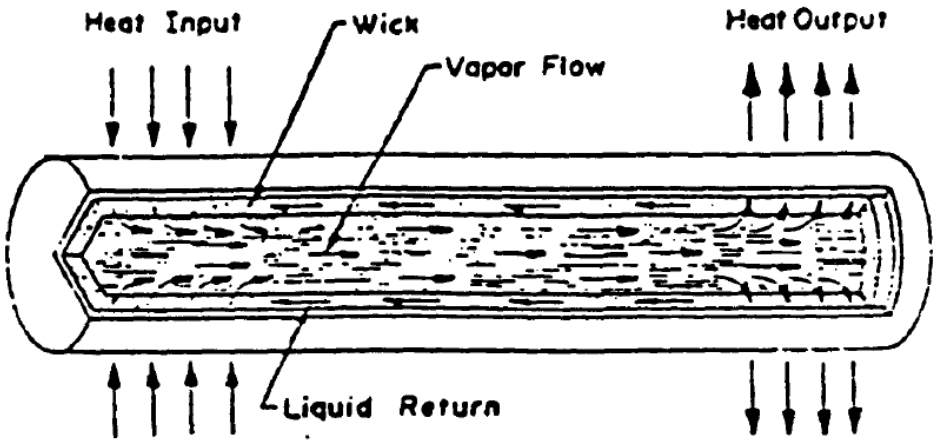

Figure 20: Scheme of heat pipe [15]

As for thermal coatings, there are various materials characterized by different absorptivity and emissivity to be applied on the MAV surface, a list is shown in the Figure 21. They are passive heat control systems [15].

Material	Absorptivity (Solar)	Emissivity (IR)
White paint	.20	.85
Black paint	.94	.94
Silvered teflon	.08	.72
Aluminum paint	.66	.20
Aluminum	.44	.08
Gold	.20	.03
Titanium	.60	.20
Beryllium	.58	.08
Steel	.85	.36

Figure 21: Absorpivities and emissivities of various materials [15]

2.3.6 Thermal Protection System

The two main sources of heat from which the MAV must be protected are the hot gases coming out of the propulsion system engines and the heat produced by the shock waves formed during ascent. Special thermal blankets called Advanced Flexible Reusable Surface Insulation (AFRSI), or protective ceramic coatings (PCCs) [14] are used to counter these problems. Other methods to counteract the heat sources may be the use of ablative materials on the MAV surface to absorb excess heat, or even the use of heat pipes and radiators already present in the MAV for TCS [15].

2.3.7 Avionic System

The avionics system corresponds to the entire electronic part of the MAV and is housed inside the crew cabin.
The avionics can be composed of several subsystems: the Command and Data Handling (C&DH), the Telemetry, Tracking and Command (TT&C), and the Guidance Navigation & Control (GN&C)
Usually, the avionics electronics are crammed into a section of the cabin that is not easily accessible to the crew, and this system is built to be as compact as possible and to take up as little space as possible.
The avionics system is critical to keep the crew in contact with the spacecraft in a parking orbit for successful rendezvous and docking, and if the expenditure in terms of mass and power is not excessive, this system can be used to stay in contact with Earth [15].
It is also used to transmit data of any kind during the mission [13].

A key part of the avionics is the on-board computer, which is the beating heart of the MAV and allows it to keep track of all the lander's various systems and report any malfunctions [15].

2.3.8 Guidance Navigation & Control

For simplicity, it will be described as an isolated system, although it is an integral part of avionics. The task of this subsystem is to track, control, and possibly adjust the trajectory of the aircraft.
This system is also responsible for monitoring the MAV during rendezvous and Docking maneuvers with the Mars Orbiting Vehicle.
All these functions are performed through a number of various instruments: inertial sensors for positioning, radar and cameras during landing and ascent, star tracking sensors, and small thrusters to enable all the various correction maneuvers (pitch, roll, lateral accelerations) to be performed [13] [15].
Usually, delta V to be provided by GN&C thrusters is at least an order of magnitude smaller than the delta V to be provided by Propulsion System engines. The propellant can be of various types and/or combinations: hydrogen peroxide, MMH-MONX, UDMH/N2O4 [18]. Both GN&C propellant and pressurizer are stowed in special tanks.

2.3.9 Electrical Power System

The EPS is responsible for producing and supplying the electrical power required by the MAV during all surface operations and during ascent. The system must meet a variety of power demands, from peaks that may occur at certain times during the mission or times when the bare minimum is required to operate the lander.

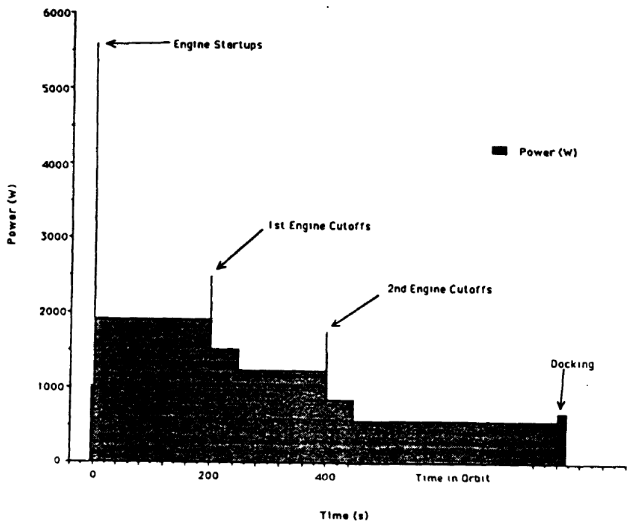

Figure 22: Example of required power

It can be seen from Figure 22 that the greatest demand for power occurs at the beginning of the ascent, while peaks are present at the time the various engines are shut down.
The main alternatives for providing electrical power to an MAV are as follows: primary batteries and fuel cells.
Batteries are the simplest electrical energy storage system to make and implement.

Battery	Specific energy (W-hr/kg)	Comments
$LiSOCl_2$	250 (NASA TM 88174, 1985)	long shelf life,best specific energy,untested
NiH_2	31.5 (MRSR, 1989)	good cycle life
AgZn	150 (NASA TM 88174, 1985)	used on all past manned space missions
NiCd	28.6 (MRSR, 1989)	low specific energy,well-tested
$LiTiS_2$	83 (MRSR, 1989)	not space proven

Figure 23: Battery comparisons

Figure 23 shows that the batteries that provide the highest specific energy are LiSOCl2 and AgZn, while the other three types of batteries are characterized by long life.
The alternative to batteries are fuel cells. They provide higher specific energy, but one might have problems in storing the gases that are used, as accidental boil off might occur. Therefore, efforts are made to avoid the use of cryogenic substances. In addition, the fuel cell system is more complicated to implement, given the presence of many more components than batteries. The most popular fuel cells are those that run on oxygen and liquid hydrogen.
As for the distribution system, the energy produced by batteries or fuel cells must first be converted to 28 V direct current. The power controller, which is monitored by a computer, determines into which system this power is to be transferred. The wiring system, consisting of cables, terminals and connectors, is used to transport the power.

Chapter 3

Statistical Analysis

This chapter will discuss a portion of the thesis work focused on collecting useful data for lander design, starting with the various configurations proposed in the literature and dividing them into subgroups based on similarity and according to other criteria that will be explained later.
Next, statistical trends will be plotted based on the various subdivisions made.
This work was carried out to achieve (to accomplish) the following objectives:

- Frame the state of the art of manned Mars landers;
- To produce a first draft methodology, so as to have a starting point for the preliminary design of the manned lander by estimating the total mass, the percentages on the dry mass of the various subsystem masses, the Thrust to be used and the delta V to be obtained;

3.1 Data collection in a database

The first step in beginning this project is the creation of two databases: one for the Mars Ascent Vehicle (MAV) and one for the landers performing Entry Descent & Landing (EDL).
This subdivision is necessary in order to extract data on the mass percentage of all MAV subsystems and then in trying to determine a weight percentage to add to the MAV dry mass related to the systems used during entry descent and landing.
This approach is critical because the goal of this thesis is to design a reusable lander that is capable of both descent and ascent through the Martian atmosphere.

3.1.1 Mars Ascent Vehicle database

The information found for writing the MAV database was classified according to different inputs, which will be listed below.

- Ascent delta V: Since the breakdown by orbit type was too coarse, it was decided to make a breakdown by ascent delta V. From the value of delta V, the sizing of the propulsion system and the calculation of the required thrust starts. Similar values of delta V, indicate similar and comparable missions.
- Mission duration: by framing the duration of the mission, one can understand the ultimate purpose of the vehicle, which ones can be compared, and which ones serve only to get an overview of the state of the art. This input also serves to get an idea of the habitable volume.
- Crew number: this parameter also helps to frame the vehicle type. There was a strong preponderance in the literature to have four people in the crew, i.e., a number that is neither too small nor too large, so as not to increase the habitable volume and weight of the ECLSS too much. There are only a few aircraft in the database that have a crew of 2 or 6 people.
- T/W ratio: the thrust-to-weight ratio is always between 0.7-1, as already anticipated in the literature review. This provides the right trade-off between generated thrust and propellant system weight.
- Propellant: most of the missions analyzed use the LOX/LCH4 combination as propellant because of the advantages in performing ISRU. LOX/LH2 and NTO/MMH combinations, hybrid propellants LOX/PARAFFINS, FFA/HNO, and oncogenic alternative propellants (ClF5/N2H4) are not so common.
- Payload mass: critical to understand how much payload can be carried, as it is one of the key requirements for these kinds of missions. In many projects this value is provided, while for others it has been estimated using statistical formulas.
- Total Mass: This figure allows identification of the type of aircraft being cataloged and its purpose, but also allows identification of maximum and minimum values within which to choose a reference aircraft. This data is used to plot statistical trends with thrust or as other masses change (dry mass, propellant mass).
- Dry mass: represents total vehicle mass minus propellant mass and payload mass. It is the most difficult mass to estimate but also one of the most significant, since it represents the sum of the masses of all the lander's subsystems.
- Inert mass: is the sum of the dry mass and the payload mass.
- Propellant mass: closely related to the type of propellant, it affects the weight of the propellant system tanks and the dry mass quite a lot.
- Thrust: mainly concerns the first stage, it is used for propulsion system sizing.

Table 1 shows an initial collection of data from MAVs that have similar delta V, same type of propellant (LOX/LCH4), but different thrust-to-weight ratios [12]. The third-to-last vehicle [20], for which only data referring to ascent have been reported, is very interesting because it is like the lander to be designed, since it performs both descent and ascent. The penultimate row [11] and the last row [17], are landers that have higher delta V, but being like each other the trend is respected.

Mission	Thrust 1st Stage [kN]	T/W	Ascent delta V (m/s)	Payload mass (kg)	Total mass (kg)	Dry mass (kg)	Inert mass (kg)	Propellant mass (kg)
TPTO to HMO	292	0.9	3777	826.77	33034	10067	10894	22967
TPTO to HMO	232	0.7	3845	826.77	33638	9239.23	10066	23572
TPTO to HMO	262	0.8	3802	826.77	33253	9239.23	10066	23187
TPTO to HMO	292	0.9	3777	826.77	33034	9240.23	10067	22967
TPTO to HMO	323	1.0	3761	826.77	32897	9240.23	10067	22830
TPTO to HMO	355	1.1	3751	826.77	32808	9240.23	10067	22741
TPTO to HMO	366	1.2	3744	826.77	31014	9239.23	10066	20948
TPTO to HMO	393	1.3	3741	826.77	30983	9239.23	10066	20917
TPTO to HMO	425	1.4	3738	826.77	30965	9238.23	10065	20900
TPTO to HMO	292	0.9	3777	826.77	33033	9240.23	10067	22966
TPTO to HMO	279	0.9	3777	676.77	32500	9340.23	10017	22483
TPTO to HMO	232	0.9	3777	826.77	33131	9338.23	10165	22967
TPTO to HMO	304	0.9	3777	1265.16	34445	9200.84	10466	23979
TPTO to HMO	309	0.9	3777	826.77	34880	9240.23	10067	24813
TPTO to HMO	292	0.9	3777	826.77	33034	9240.23	10067	22967
TPTO to HMO	279	0.9	3777	826.77	31528	9239.23	10066	21462
TPTO to HMO	231	0.7	3845	826.77	33639	9240.23	10067	23572
TPTO to LMO	230	0.9	3777	802.28	25981	9170.72	9973	16008
TPTO to LMO	251	1.0	3766	802.28	25496	9170.72	9973	15523
TPTO to HMO	371		4698	783.11	60808	15700	16483	45108
TPTO to HMO	235	1.8	5137	792.0033	36152	8649	9441	26478
TPTO to HMO	300		5413	1106.00	42900	8894	10000	32900

Table 1: LOX/LCH4 Mission Data Table (MAV)

Table 2 shows all the other MAVs that use different types of propellants and are therefore impossible to correlate with all the other MAVs in Table 4. These have been represented as individual points within the graphs that will be shown next, with the sole purpose of framing the state of the art [11] [12] [14].

Mission	Thrust 1st Stage [kN]	T/W0.9	Propellant	Ascent delta V (m/s)	Payload mass (kg)	Total mass (kg)	Dry mass (kg)	Inert mass (kg)	Propellant mass (kg)
TPTO to HMO	330	0.9	NTO/MMH	3777	826.77	37332	9239.23	10066	27266
TPTO to HMO	230	0.9	LOX/LH2	3777	826.77	36082	9240.23	10067	16015
TPTO to HMO	375		LOX/PAR.WAX	5274	635.00	6749	3426	4061	2688
TPTO to HMO	175	1.8	CIF5/N2H4	5137	792.00	27188	6315	7107	20081

Table 2: Other propellants and atypical Missions Data Table (MAV)

While two-stage MAVs were analyzed in the previous two, data inherent to single-stage MAVs were collected in Table 3 and Table 4. This solution is quite discouraged as the weight of the lander increases since it is impossible to exploit the advantages of staging, consequently few examples can be found in the literature. Even with a single stage, most configurations feature the LOX/LCH4 combination, while other configurations with more advanced alternative propellants are also present [12] [15] [16] [17] [18] [19].

Mission	Thrust [kN]	T/W	Propellant	Delta V (m/s)	Payload mass (kg)	Total mass (kg)	Dry mass (kg)	Inert mass (kg)	Propellant mass (kg)
SPTO to HMO	410	0.9	LOX/LCH4	4016	826.77	46224	10195	11022	35202
SPTO to HMO	315	0.7	LOX/LCH4	4036	827.77	45966	10195	11022	34944
SPTO to LMO	295	0.9	LOX/LCH4	4016	802.28	33300	9264.72	10067	23233
SSTO to LMO	101		LOX/LCH4	5700	833.23	18000	3166.77	4000	14000

Table 3: Single Stage LOX/LCH4 Missions Data Table (MAV)

Mission	Thrust [kN]	Propellant	Delta V (m/s)	Payload mass (kg)	Total mass (kg)	Dry mass (kg)	Inert mass (kg)	Propellant mass (kg)
SSTO to HMO	135	NTO/MMH	5209	140	14093	2620.5	2760.5	11332.5
SSTO to LMO	300	NTO/MMH	4176	1049	24400	4951	6000	18400
SSTO to LMO	72	FFA/HNO3	4830	212	4190	580	792	3398
SSTO to LMO	250	MMH/MON25	4200	982	26292	6632	7614	18678

Table 4: Single Stage Other Propellants Missions Data Table (MAV)

3.1.2 Mars Ascent Vehicle database graphs

Once all the data from the various MAVs have been collected within the tables presented in the previous section, the graphs are plotted using and comparing the most useful design variables. In addition, in the graphs, regression lines were drawn for the variables between similar architectures.
Figure 24 shows the trend of total mass versus payload mass for the various MAVs and regression lines were plotted grouped by mission type (delta V, number of stages, propellant). Regression lines equations are reported in Table 5 where y is the total mass.
Taking payload mass as input, which is one of the main design parameters, an initial estimate of the total mass that the MAV will have can be derived.

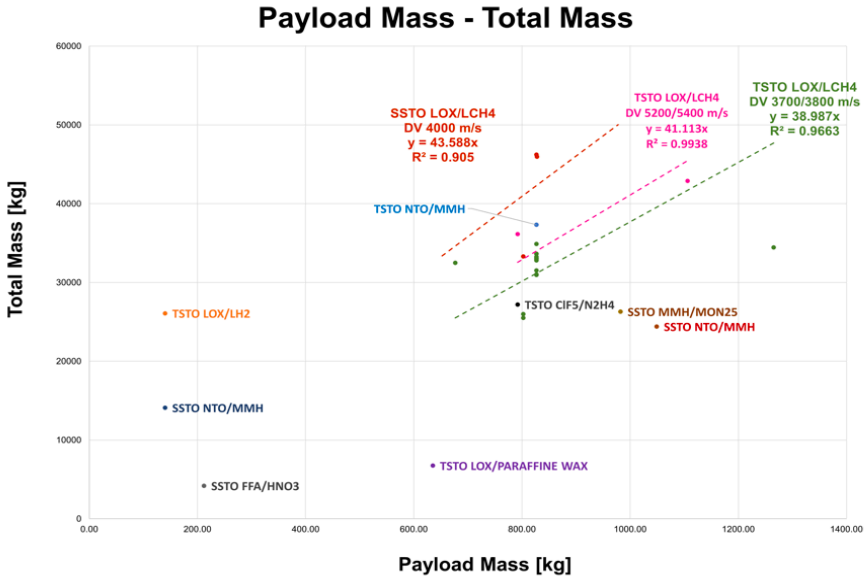

Figure 24: MAV Statistical Trends: Payload Mass - Total Mass

Myssion Type	Delta V (m/s)	**Equation** y	R^2
SSTO LOX/LCH4	4000	y = 43.588x	0.905
TSTO LOX/LCH4	5200/5400	y = 41.113x	0.9938
TSTO LOX/LCH4	3700/3800	y = 38.987x	0.9663

Table 5: MAV Statistical Equations: Payload Mass - Total Mass

The same thing was done in Figure 25, only instead of total mass, dry mass was put on the y-axis. Again, by entering the payload mass as input, an initial estimate of the MAV dry mass can be obtained.
Regression lines equations are reported in Table 6 where y is the dry mass.

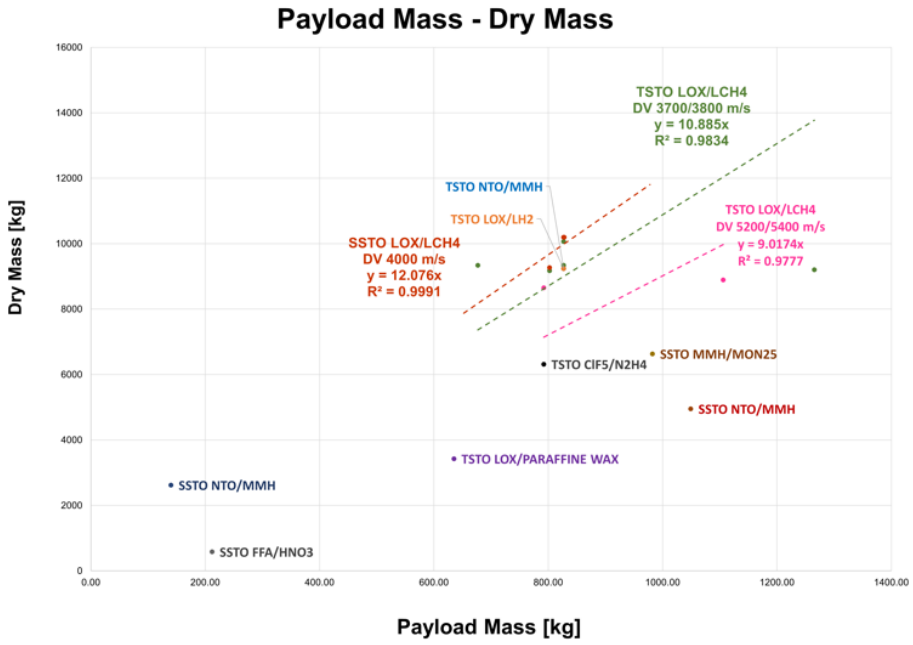

Figure 25: MAV Statistical Trends: Payload Mass - Dry Mass

Myssion Type	Delta V	**Equation** y	R^2
SSTO LOX/LCH4	4000	y = 12.076x	0.9991
TSTO LOX/LCH4	5200/5400	y = 9.0174x	0.9777
TSTO LOX/LCH4	3700/3800	y = 10.885x	0.9834

Table 6: MAV Statistical Equations: Payload Mass - Dry Mass

Figure 26 shows the thrust of the first stage as the total mass of the MAV varies. Depending on the total mass obtained, an initial estimate of the thrust required to perform the ascent can be obtained. Again, regression lines were plotted by grouping by mission type (delta V, number of stages, propellant).
Regression lines equations are reported in Table 7 where y is the Thrust.

Myssion Type	Delta V	**Equation** y	R^2
SSTO LOX/LCH4	4000	y = 0.0081x	0.986
TSTO LOX/LCH4	5200/5400	y = 0.0068x	0.9986
TSTO LOX/LCH4	3700/3800	y = 0.0093x	0.9677

Table 7: MAV Statistical Equations: Total Mass – Thrust

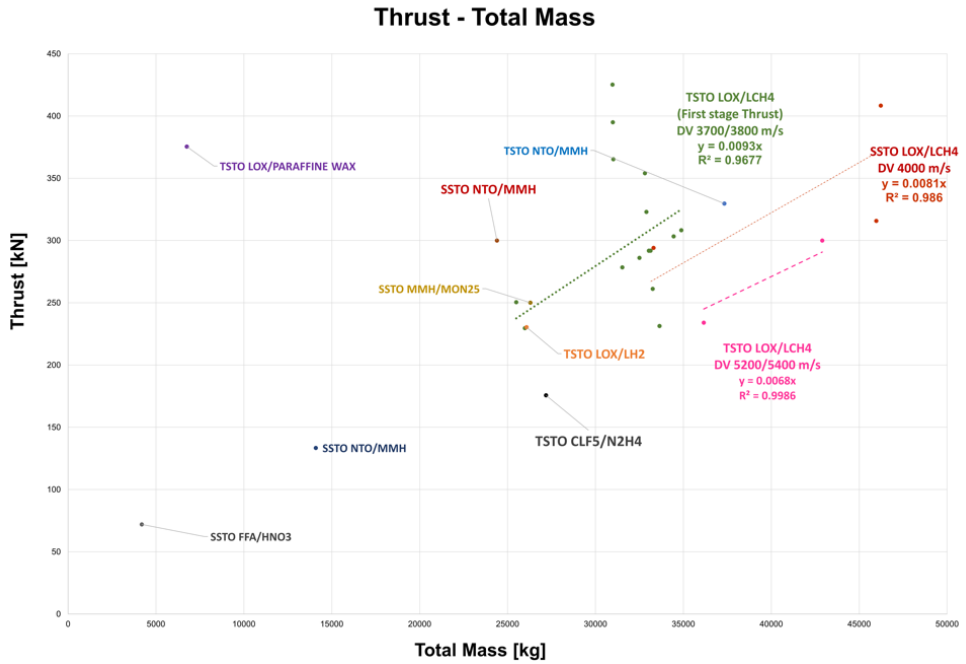

Figure 26: MAV Statistical Trends: Total Mass - Thrust

It should be emphasized that to obtain a truthful output, it is essential to group similar missions together, which prevents a broad statistical base. Numerous architectures have been included to provide a comprehensive overview of the state of the art of manned missions to Mars. This approach will allow the MAV design, derived from this thesis, to be contextualized within this analysis, contributing to a more comprehensive view.

3.1.3 Entry Descent Landing Database

To complete the statistical analysis, the database of missions that include EDL is compiled. In fact, the MAV is not equipped with the various systems that can make up the TPS of a lander that also performs EDL, since the operations and temperatures to be addressed are different. These systems can be multiple and were analyzed in section *2.2 Mars Entry Descent & Landing.* To get an initial estimate of the masses that characterize the various TPSs, all missions regarding EDL found in the literature were analyzed.
The mass data are categorized as follows:

- Total Mass: from Table 8 it can be seen that they are much higher than those found in the MAV database, this is because many lander configurations also contain inside ascent modules, rovers, cargo that will be used in the later phases of the simulated missions;
- Dry Mass: for the reasons listed before, dry masses are also higher than those found in the MAV database;
- TPS & Deceleration System Masses: masses of the various systems used to perform the EDL and main data that wants to be found through the creation of this database.

TPS & Deceleration System Mass [kg]	Total Mass [kg]	Dry Mass [kg]
4608	62791	21565
6706	77516	26280
6000	109000	57400
25700	133500	84700
8658	60435	21355
3762	57233	20190
5499	63921	27937
6373	75000	26270
7025	68277	19781
6800	62000	40190
3025	41715	25815

Table 8: EDL Mass Distribution [7][18][20][21][22][23][24]

3.1.4 Entry Descent Landing database graphs

In Figure 27 and Figure 28, the mass values of the TPS+Deceleration system along with the total mass and dry mass are shown graphically. In both graphs, regression lines are plotted to extrapolate a mass percentage on both the dry mass and total mass of the systems used for THE EDL. The equations are shown in Table 9.
Several technologies used for EDL are included in both graphs and were discussed earlier in Chapter 2.
These graphs, therefore, provide both an overview of the state of the art of these technologies and a first rough estimate of the percentage by weight to be added to our MAV to also consider the systems to be used for descent through the Martian atmosphere.
In the next chapter, one of these technologies will be discussed and chosen to build the TPS that will characterize the Martian manned lander.

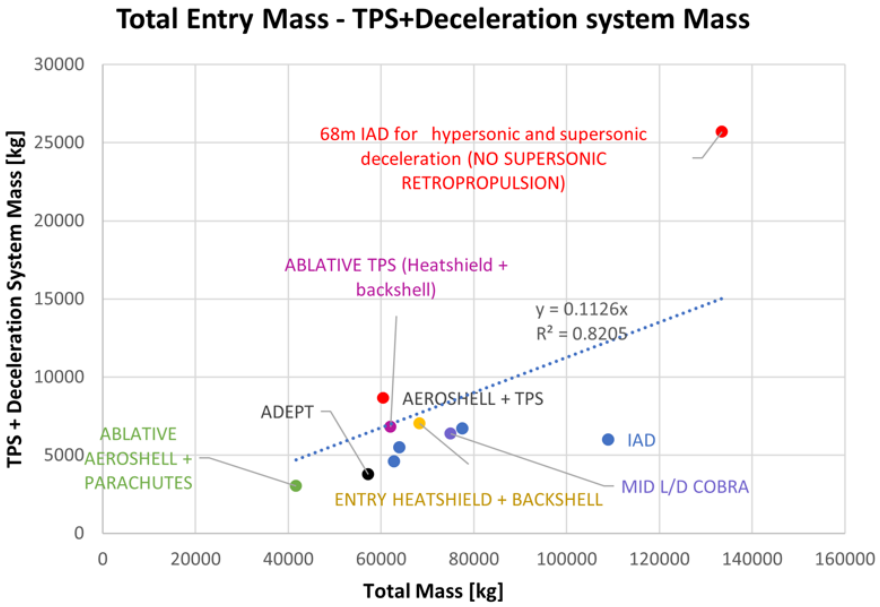

Figure 27: TPS + Deceleration System Mass - Total Mass

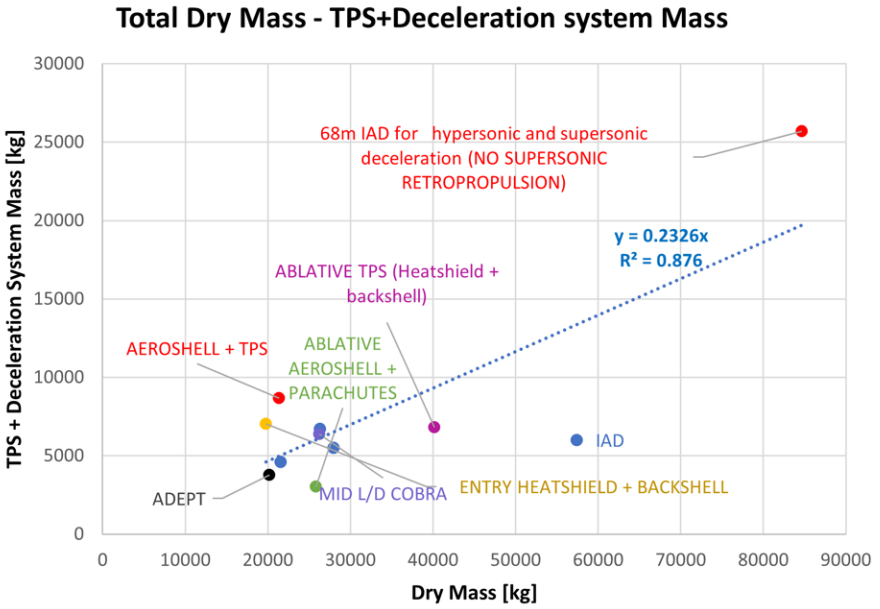

Figure 28: TPS + Deceleration System Mass - Dry Mass

Investigated mass	**Equation** y	R^2
Total Mass	y = 0.1126x	0.8205
Dry Mass	y = 2326x	0.876

Table 9: EDL Statistical equation: Dry Mass/Total Mass – TPS & Dec. Sys Mass

3.2 First Design Methodology & Starting Point for Subsystem Design

From the 'statistical analysis performed, an initial design methodology can be derived, shown in Figure 29.
From the datasheets of the various documents used in the previous chapters, it is possible to estimate the mass percentages on the dry mass of all lander subsystems, including the TPS used to perform the EDL. By integrating this information with another design methodology regarding multipurpose landers found in the book reference [25], the percentages in the figure below were obtained.

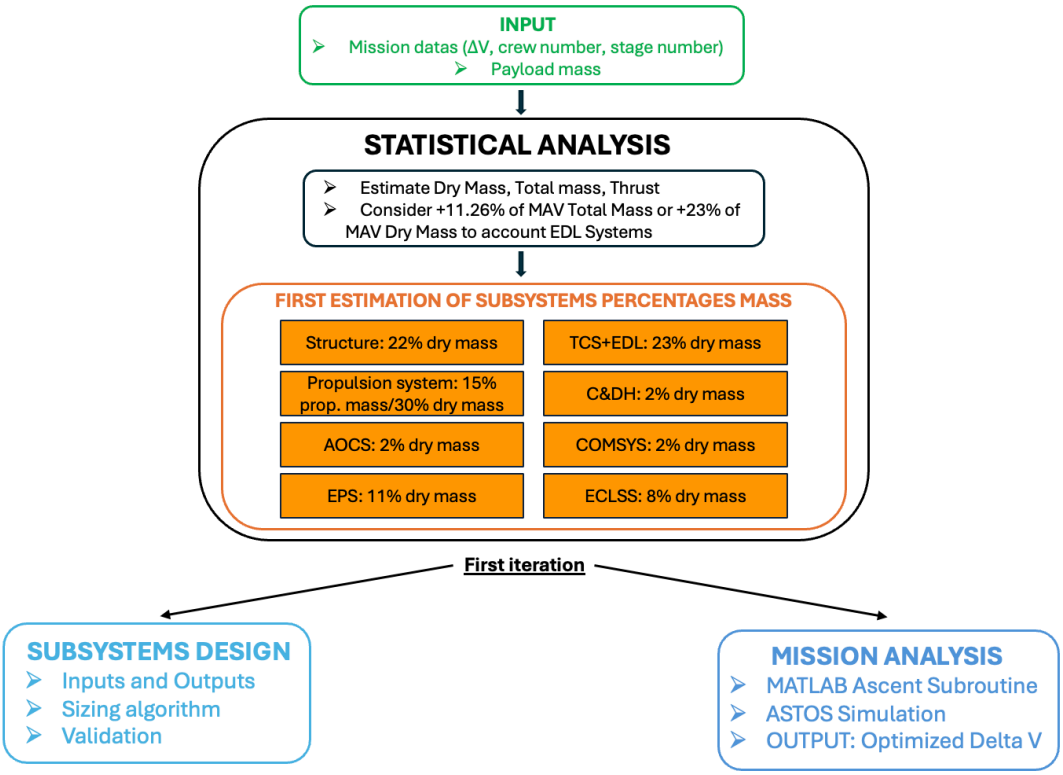

Figure 29: Statistical analysis summary work & next steps

The methodology obtained at the end of the statistical analysis serves to have a clear starting point regarding the first iteration of the Subsystem Design work that will be done in this thesis and the Mission Analisys work that will be done in parallel in another thesis.
Regarding the Subsystem design work, the percentages found are used to get a first idea of the mass of the various subsystems, later these percentages will be updated as the 'work progresses. Other data, such as the Thrust required for the MAV and the delta V useful to reach the final parking orbit, were

obtained from the statistical analysis and used for the propulsion system sizing. These aspects will be discussed in more detail in *Subsystem Design*

Chapter 4

Subsystem Design

This chapter will discuss all the subsystems that make up the lander that is to be designed. As mentioned earlier, the MAV will be capable of descent using the TPS and ascent. After giving a description of the composition and functions of the individual subsystem, a series of inputs will be given that the user must select for the listed outputs to be obtained. In particular, the value of the outputs in this paper was obtained by choosing ad hoc inputs to have an initial sizing of the lander. Next, the algorithm for each subsystem will be presented, listing the various assumptions made and the formulas used so that the desired outputs are obtained.

4.1 Optimal Staging

The Optimal Staging algorithm used within this thesis allows for the calculation of the minimum Maximum Take Off Weight (MTOW) of a MAV to make the ascent from the Martian soil using the following set of inputs:

1. Number of stages [-];
2. Payload mass [kg];
3. Altitude of target orbit [km];
4. The vacuum specific impulse [s];
5. Structural ratio [-];
6. Delta V [m/s].

The payload mass, the altitude of target orbit and delta V are inputs chosen based on the statistical analysis performed in the previous chapter.

The algorithm has the function of calculating the minimum MTOW and propellant mass for a vehicle with N stages to ascend from the Martian soil with a given payload mass. After calculating the MTOW and propellant mass, the dry mass is derived, which will be used as data for the first sizing of the subsystems that will compose the lander and will be updated at the end of each iteration.

The input values that will be considered ad hoc to initiate lander sizing are as follows:

1. 2 stages.

2. 900 kg of payload mass.
3. 500 km circular orbit.
4. LOX/LCH4 as a propellant.
   i) Vacuum Isp: 360 s
5. 0.45 and 0.55 structural ratio for first and second stage.
6. 4000 m/s of required delta V.

Following the algorithm explained in [26] , the outputs obtained are:

1. MTOW: 45304 kg
2. Propellant mass: 23990 kg
3. Dry mass: 21315 kg

These outputs will be used to perform calculations in some subsystems.

4.2 Attitude & Orbit Control System

The Attitude & Orbit Control System (AOCS) is fundamental for stabilizing and orienting the vehicle in the desired directions during the various phases of the mission. For the Human Landing System is very important for the ascend and descent phases [25]. AOCS must perform the following functions:

1. variation of the lander's velocity vector in terms of modulus and/or direction through use of thrusters that generate a controlling force that consumes propellant.
2. Determination of the position, orientation and speed of the lander
3. Generation of control commands to follow the desired trajectory.
4. Control of trajectory correction maneuvers during descent.

The only steps considered for sizing are as follows: descent, ascent and docking, while detumbling is not considered for sizing.

4.2.1 Inputs & Outputs

Below, a set of inputs will be listed that the user must choose for the outputs listed through the sizing algorithm to be obtained.

INPUT

1. Propellant type [-]
   i) Isp [s]
   ii) Density $\left[\frac{kg}{m^3}\right]$
2. Delta V for aocs manouvers [m/s]
3. Mixture ratio [-]

4. Tank material [-]
   i) Yield tension [Pa]
   ii) Density $\left[\frac{kg}{m^3}\right]$
5. Number of tanks [-]

OUTPUT

1. Total AOCS mass: 2424.1 kg
2. Propellant mass: 2186.7 kg
3. Tanks mass (oxydizer + fuel): 122.02 kg
4. Total propellant volume: 1.8681 m^3

4.2.2 Sizing Algorithm

All the formulas used for sizing this subsystem will be listed below.

Propellant

The Tsiolkovsky eq. (4.1) is used to calculate the mass of propellant that will be used to perform the AOCS maneuvers.

$$\boldsymbol{m_p} = MTO_{mass} \cdot \left(1 - exp\left(-\frac{\Delta V}{Isp \cdot g_{Earth}}\right)\right) \quad (4.1)$$

Where:

- ΔV [m/s] is the delta V for the AOCS manouvers
- Isp [s] is the specific impulse of AOCS propellant

To have an initial estimate of the mass of the AOCS, the MMH/MON-3 combination is assumed to be used as the propellant [27].

- Isp = 340 m/s
- MMH density = 880 $\frac{kg}{m^3}$
- MON-3 density = 1370 $\frac{kg}{m^3}$

The oxydizer mass [kg] can be calculated by using eq. (4.2), while the fuel mass [kg] with eq. (4.3):

$$m_{ox} = m_p \cdot 0.694 \quad (4.2)$$

$$m_{fuel} = m_p \cdot 0.306 \quad (4.3)$$

The volume of oxydizer [m^3] can be calculated by using eq. (4.4), while fuel volume with eq. [m^3] eq. (4.5):

$$V_{ox} = m_{ox}/\rho_{MMH/MON3} \quad (4.4)$$

$$V_{fuel} = m_{fuel}/\rho_{MMH/MON3} \quad (4.5)$$

Propellant volume $[m^3]$ is given by the sum of fuel and oxidizer volume, as written in eq. (4.6):

$$\boldsymbol{V_{prop}} = V_{ox} + V_{fuel} \quad (4.6)$$

Spherical tank sizing for oxydizer and fuel: Spherical tank

Spherical reservoirs have a uniform distribution of stress over the entire surface, this makes them very robust and able to withstand high loads.

The formulas that make up the algorithm for spherical tanks will be listed below [28]. The same algorithm will also be used in the paragraph of ECLSS, Propulsion System, TPS and EPS.

Tank radius of oxidizer/fuel [m] is calculated with eq. (4.7), while the thickness [m] with eq. (4.8):

$$r_{tank_{ox/fuel}} = \sqrt[3]{\frac{3}{4} \cdot \frac{V_{ox/fuel}/_N}{\pi}} \quad (4.7)$$

$$t_{tank_{ox/fuel}} = \frac{sf \cdot P_{BOL} \cdot r_{tank_{ox/fuel}}}{2\sigma_y} \quad (4.8)$$

Where:

- Safety factor: $sf = 2$.
- N is tanks number
- Beginning of life pression: $P_{BOL} = 2.4 \cdot 10^6 Pa$.
- Yield tension of material tank: σ_y.

Oxydizer/fuel tank Volume $[m^3]$ and Mass [kg] can be calculated with eq. (4.9) and eq. (4.10):

$$V_{tank_{ox/fuel}} = \frac{4}{3} \cdot (r_{tank_{ox/fuel}} + t_{tank_{ox/fuel}})^3 - V_{ox/fuel} \quad (4.9)$$

$$m_{tank_{ox/fuel}} = V_{tank_{ox/fuel}} \cdot \rho_{material} \quad (4.10)$$

Total mass AOCS tank [kg] is sum of fuel tank mass fuel and oxidizer tank eq. (4.11):

$$\boldsymbol{m_{tank_{tot}}} = m_{tank_{fuel}} + m_{tank_{ox}} \quad (4.11)$$

Where:

- $\rho_{material}$ is tank material density

AOCS total mass [kg] is sum of all component mass previously calculated with margin of 5% as shown in eq. (4.12):

$$\boldsymbol{m_{tot}} = (m_{tank_{fuel}} + m_{tank_{ox}} + m_{ox} + m_{fuel}) \cdot 1.05 \quad (4.12)$$

Cylindrical Tank for oxydizer and fuel

Cylindrical tanks, have a smaller footprint than spherical tanks, fit better in the available space, but stress distribution is not uniform. The formulas that make up the algorithm for cylindrical tanks will be listed below [27]. The same algorithm will also be used in the paragraph of ECLSS and Propulsion System.

The cylindrical tank is considered with hemispherical domes.

Entering the length of the cylinder (L) as input, the tank radius of oxidizer/fuel is calculated [m] with eq. (4.13):

$$r_{tank_{ox/fuel}} = \sqrt{\frac{V_{ox/fuel}}{L \cdot N \cdot \pi}} \quad (4.13)$$

Where:

- N is tanks number

Depending on the case and space availability within the lander, the user chooses to put the radius as an input as well.

Oxydizer/fuel tank thickness [m] and mass [kg] can be calculated with eq. (4.14 and eq. (4.15):

$$t_{tank_{ox/fuel}} = \frac{1.5 \cdot P_{BOL} \cdot r_{tank_{ox/fuel}}}{\sigma_y} \quad (4.14)$$

$$m_{tank_{ox/fuel}} = N \cdot 2 \cdot \pi \cdot L \cdot r_{tank_{ox/fuel}} \cdot t_{tank_{ox/fuel}} \cdot \rho_{material} \quad (4.15)$$

Where:

- Beginning of life pression: $P_{BOL} = 2.4 \cdot 10^6 Pa$.
- Yield tension of material tank: σ_y.
- $\rho_{material}$ is tank material density

Total mass AOCS cilyndrical tank [kg] is sum of fuel tank mass fuel and oxidizer tank eq. (4.16):

$$\boldsymbol{m_{tank_{tot}}} = m_{tank_{fuel}} + m_{tank_{ox}} \quad (4.16)$$

4.3 Environmental Control & Life Support System

Environmental Control & Life Support system (ECLSS) is the subsystem whose main objective is to provide an adequate environment for human survival. This is done by controlling atmospheric parameters, providing resources, and managing waste products to support the lives of the astronauts and provide them with the necessary comfort so that they can carry out their mission [25].
The ECLSS, to provide a livable environment, must perform the following tasks:

- Provide the correct air pressure, temperature, humidity and composition to the pressurized volume of the lander by removing carbon dioxide, contaminants and providing oxygen and nitrogen.
- Respond promptly to unanticipated failure situations.
- Provide life-sustaining resources such as food, water and air.
- Managing solid and liquid wastes.

This thesis will focus mainly on the Enviromental Control part, which is responsible for keeping the crew in standard conditions.
Enviromental Control, consists of four different systems:

1. Air Revitalization System (ARS), which is responsible for removing carbon dioxide, generating oxygen, controlling trace contaminants, and monitoring the main constituents of the cabin atmosphere.
2. Atmosphere Control and Supply (ACS), which is primarily concerned with controlling the pressure and composition of the atmosphere, responding to pressure changes, and supplying oxygen and gases to the astronauts and utilities.
3. Fire Detection and Suppression (FDS), which deals with smoke detection and fire detection and suppression.

4. Thermal and Humidity Control (THC), which mainly focuses on controlling the humidity present within the atmosphere and the thermal conditions of the equipment and crew.

The Life Support part, i.e., all components concerning the management and discarding of water, food, and waste was not addressed within this thesis [29][30].

4.3.1 Inputs & Outputs

INPUT

1. Number of crew members [-]
2. Residence time inside the lander [day]
3. Type of atmosphere (Oxygen, Nitrogen and Air molar mass) [-]

OUTPUT

1. Total ECLSS mass (with components): 713.81 kg
2. Habitable Volume: 7.765 m^3
3. Pressurized volume: 12.95 m^3
4. Total mass oxygen: 5.62 kg
5. Total mass oxygen tank: 2.16 kg
6. Total volume oxygen gas: 0.4337 m^3
7. Total volume oxygen tank: 0.1665 m^3
8. Total mass nitrogen: 12.49 kg
9. Total mass nitrogen tank: 21.23 kg
10. Total volume nitrogen: 0.0129 m^3

SPHERICAL TANK: from (4.33) to (4.36)

1. Total mass oxygen tank: 2.35 kg
2. Total volume oxygen tank: 0.000868 m^3
3. Total mass nitrogen tank: 8.62 kg
4. Total volume nitrogen tank: 0.0032 m^3

COMPONENTS

1. Total mass: 672.31 kg
2. Total Volume: 1.7955 m^3
3. Total Power: 3112.9 W

4.3.2 Sizing Algorithm

Air supplies

Habitable volume [m^3] according to Celentano study [31] with the eq. (4.17):

$$\boldsymbol{V_{habitable}} = n_{crew} \cdot 20 \cdot \left(1 - \ exp\left(-\frac{n_{days}}{20}\right)\right) \quad (4.17)$$

Where:

- n_{crew}: number of crew.
- n_{days}: number of days.

Total air needed $\left[\frac{\frac{Kg}{pers}}{day}\right]$ and total volume of air $[m^3]$ can be calculated with eqs. (4.18) and (4.19):

$$Air_{need} = r_{data} \cdot n_{crew} \cdot n_{days} \quad (4.18)$$

$$V_{tot_{air}} = 7.772 \cdot 10^{-2} \cdot Air_{need} \quad (4.19)$$

Where:

- Respiration data –> kg of air needed by person for a day: $r_{data} = 0.84 \frac{kg}{\frac{pers}{day}}$.

The habitable volume is assumed to be 60% of the pressurized volume [32], so with eq. (4.20) it can be calculated:

$$\boldsymbol{V_{pressurized}} = \frac{V_{habitable}}{0.6} \quad (4.20)$$

Total number air Mole is calculated with eq. (4.21):

$$Mol_{tot\ air} = p_{eclss} \cdot \left(\frac{V_{pressurized}}{R_{gas} \cdot T_{eclss}}\right) + Air_{need} \cdot \frac{1000}{MM_{air}} \quad (4.21)$$

Where:

- Pressure inside enviroment: $p_{eclss} = 65500\ Pa$.
- Temperature inside enviroment: $T_{eclss} = 293\ K$.

Oxygen Supplies

Number of Oxygen Mole can be calculated with eq. (4.22):

$$Mol_{ox} = Mol_{tot\ air} \cdot Ox_{conc} \quad (4.22)$$

Where:

- Oxygen concentration: $Ox_{conc} = 30\%$.

Total Oxygen volume $[m^3]$, can be calculated using eq. (4.23), while the Mass [kg] with eq. (4.24):

$$V_{ox} = V_{habitable} \cdot Ox_{conc}/100 \quad (4.23)$$

$$\boldsymbol{m_{ox}} = MM_{ox} \cdot Mol_{ox} \quad (4.24)$$

Total Oxygen tank Mass [kg] and Volume $[m^3]$ can be calculated with eqs. (4.25) and (4.26):

$$\boldsymbol{m_{tank_{ox}}} = m_{ox} \cdot 0.384 \quad (4.25)$$

$$\boldsymbol{V_{tank_{ox}}} = 7.72 \cdot 10^{-2} \cdot m_{tank_{ox}} \quad (4.26)$$

Finally, with eq. (4.27) Total Volume of Oxygen gas $[m^3]$ can be calculated:

$$\boldsymbol{V_{tot_{ox}}} = 7.72 \cdot 10^{-2} \cdot m_{ox} \quad (4.27)$$

Where:

- The cabin was filled with air -> 70% nitrogen, 30% oxygen [33]

Nitrogen supplies

Total Nitrogen moles can be calculated with eq. (4.28):

$$Mol_{N2} = Mol_{tot\ air} - Mol_{ox} \quad (4.28)$$

The Nitrogen mass [kg] considering leaks can be calculated by using eq. (4.29) while nitrogen mass tank with eq. (4.30):

$$\boldsymbol{m_{N2}} = N2_{leak} \cdot Mol_{N2} \cdot n_{days} \cdot MM_{N2} \quad (4.29)$$

$$\boldsymbol{m_{tank_{N2}}} = m_{N2} \cdot 1.7 \quad (4.30)$$

The total mass [kg] of nitrogen supplies (gas + tank) can be calculated by usine eq. (4.31), while total Nitrogen volume is given by eq. (4.32):

$$m_{tot_{N2}} = m_{N2} + m_{tank_{N2}} \quad (4.31)$$

$$\boldsymbol{V_{tot_{N2}}} = m_{tot} \cdot MM_{air} \cdot \frac{T_{N2}}{2.3 \cdot 10^7} \quad (4.32)$$

Where:

- Percentage of N2 leakages: $N2_{leak} = 0.5\%$.

- N2 temperature: $T_{N2} = 303\ K$.

Spherical tank sizing for Oxygen and Nitrogen
Oxygen/N2 tank radius [m] and thickness [m] can be calculated by using eqs. (4.33) and (4.34):

$$r_{tank_{ox/N2}} = \sqrt[3]{\frac{3}{4} \cdot \frac{V_{ox/N2}/_N}{\pi}} \quad (4.33)$$

$$t_{tank_{ox/N2}} = \frac{sf \cdot P_{tank_{ox/N2}} \cdot r_{tank_{ox/N2}}}{2\sigma_y} \quad (4.34)$$

Where:
- N is tanks number
- Pressure inside N2 tank: $P_{tank_{N2}} = 2.3 \cdot 10^7 Pa$.
- Pressure inside oxygen tank: $P_{tank_{ox}} = 200000\ Pa$.
- Safety factor: $sf = 2$.
- Yield tension of material tank: σ_y.

Oxygen/N2 tank radius Volume [m^3] and tank mass [kg] is given by eqs. (4.35) and (4.36):

$$\boldsymbol{V_{tank_{ox/N2}}} = \frac{4}{3} \cdot (r_{tank_{ox/N2}} + t_{tank_{ox/N2}})^3 - V_{ox/N2} \quad (4.35)$$

$$\boldsymbol{m_{tank_{ox/N2}}} = V_{tank_{ox/N2}} \cdot \rho_{material} \quad (4.36)$$

Where:
- $\rho_{material}$ is tank material density

Cylindrical Tank for Oxygen and N2
The cylindrical tank is considered with hemispherical domes.
Entering the length of the cylinder (L) as input, the Oxygen/N2 tank radius [m] and thickness are calculated [m] with eqs. (4.37) and (**Errore. L'origine riferimento non è stata trovata.**:

$$r_{tank_{ox/N2}} = \sqrt{\frac{V_{ox/N2}}{L \cdot N \cdot \pi}} \quad (4.37)$$

$$t_{tank_{ox/N2}} = \frac{1.5 \cdot P_{tank\ ox/N2} \cdot r_{tank_{ox/N2}}}{\sigma_y} \quad (4.38)$$

Where:

- N is tanks number
- Pressure inside N2 tank: $P_{tank_{N2}} = 2.3 \cdot 10^7 Pa.$
- Pressure inside oxygen tank: $P_{tank_{ox}} = 200000\ Pa.$
- Yield tension of material tank: σ_y.

Depending on the case and space availability within the lander, the user chooses to put the radius as an input as well.

Oxygen/N2 tank mass [kg] value is given by eq. (4.39):

$$m_{tank_{ox/N2}} = N \cdot 2 \cdot \pi \cdot L \cdot r_{tank_{ox/N2}} \cdot t_{tank_{ox/N2}} \cdot \rho_{material} \quad (4.39)$$

Where:

- $\rho_{material}$ is tank material density

Mass, power and volume of all components

The most important components for Environmental Control that are considered are:

- 1 CO2 Scrubber, a component that absorb CO2 with LiOH canisters.
- 1 TCCS (Trace Contaminant Control Subsystem).
- 1 OGA (Oxygen Generation Assembly), that is a Water Electrolyzer which takes water as input from the Water Recovery System and provides as output O2 to the cabin and H2 to other components.

Mass [kg], Volume [m^3] and Power [W] of CO2 Scrubber are calculated with eqs. (4.40), (4.41) and (4.42):

$$m_{scrubber} = 1.75 \cdot n_{crew} \cdot n_{days} \quad (4.40)$$

$$V_{scrubber} = 0.00123 \cdot n_{crew} \cdot n_{days} \quad (4.41)$$

$$P_{tot\,scrubber} = P_{scrubber} \cdot n_{crew} \quad (4.42)$$

Mass [kg], Volume [m^3] and Power [W] of CO2 Scrubber, TCCS and OGA are given by eqs. (4.43, (4.44) and (4.45):

$$m_{tot} = m_{scrubber} + m_{TCCS} + m_{OGA} \quad (4.43)$$

$$V_{tot} = V_{scrubber} + V_{TCCS} + V_{OGA} \quad (4.44)$$

$$P_{tot} = P_{scrubber} + P_{TCCS} + P_{OGA} \quad (4.45)$$

Where m_{TCCS}, m_{OGA}, V_{TCCS}, V_{OGA}, P_{TCCS}, P_{OGA} are taken from table 17-9 of [25].

To consider the other components outside those already considered above, we add a % margin. This margin was calculated by calculating the mass, volume and power of all the various components of the ECLSS used in [20]. Total components mass [kg], volume [m^3] and power [W] can be calculated with eqs. (4.46), (4.47) and (4.48):

$$\boldsymbol{m_{tot\ comp}} = (m_{tot} + m_{tot} \cdot 1.74) \cdot 1.05 \quad (4.46)$$

$$\boldsymbol{V_{tot\ comp}} = (V_{tot} + V_{tot} \cdot 1.34) \cdot 1.05 \quad (4.47)$$

$$\boldsymbol{P_{tot\ comp}} = (P_{tot} + P_{tot} \cdot 0.84) \cdot 1.05 \quad (4.48)$$

4.4 Propulsion System

The Propulsion System has the fundamental task of providing the lander with the necessary thrust to make the descent to the Martian soil using retro-propulsion and to make the ascent to the parking orbit [25].
The use of a bipropellant chemical Propulsion System, i.e., composed of an oxidizer and a fuel, was chosen for this lander.
The propellant is sent into the combustion chamber, which reacts to produce hot gases that are expanded and accelerated in a nozzle, causing the lander to increase speed.
Chemical propulsion was chosen over other types for a variety of reasons:

1. Chemical propulsion is usually used when the delta V to be provided is high (>1000 m/s).
2. The technology used is in common use in most space applications, so this type of propulsion is the most tested, safe and reliable.
3. With current technologies, the thrust provided by electric propulsion would not be sufficient to make the ascent from Mars while nuclear propulsion is still too immature to be used in our case study [28].

For the lander design, the main assumption made is that the engines used for descent and ascent are the same.

4.4.1 Inputs & Outputs

INPUT

1. Engines number [-]
2. Delta V [m/s]
3. Propellant type
   i) Isp [s]
   ii) Density $\left[\frac{kg}{m^3}\right]$
4. Propellant mass from optimal staging [kg]
5. Mixture ratio [-]
6. Tanks number [-]
7. Tanks material [-]
   i) Yield tension [Pa]
   ii) Density $\left[\frac{kg}{m^3}\right]$
8. Pressurant type [-]
   i) Density $\left[\frac{kg}{m^3}\right]$

OUTPUT

1. Total PS mass: 5281.52 kg
2. Total mass engine: 1313.3 kg
3. Fuel mass: 5331.1 kg
4. Oxydizer mass: 18659 kg
5. Fuel tank mass: 903.43 kg
6. Oxydizer tank mass: 1176 kg
7. Total pressurant mass: 548.91 kg
8. Total volume pressurant: 2.7363 m^3
9. Tank mass pressurant for oxydizer: 925.96 kg
10. Tank mass pressurant for fuel: 711.32 kg

4.4.2 Sizing Algorithm

Engines mass

Single engine mass [kg] can be calculated by usign eq. (4.49), the value that comes out is multiplied by the number of engines in eq. (4.50) to get the total engines mass [kg]:

$$m_{single\ engine} = 0.0135 \cdot n_{engine}^{0.4118} \cdot m_{prop}^{0.3574} \cdot Thrust_{single\ engine}^{0.471} \quad (4.49)$$

$$\boldsymbol{m_{tot\ engine}} = n_{engine} \cdot m_{single\ engine} \quad (4.50)$$

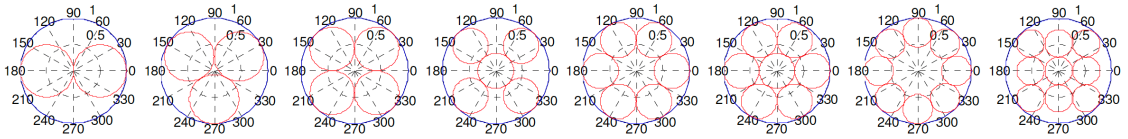

Figure 30: Geometrical configuration for engine assemblies with Number engine>1

In Figure 30 arrangements according to the number of engines are represented [34].

Spherical tank sizing for propellant

Oxydizer mass [kg] and fuel mass, can be obtained by using eqs. (4.51) and (4.52):

$$\boldsymbol{m_{ox}} = m_{prop} - m_{fuel} \quad (4.51)$$

$$\boldsymbol{m_{fuel}} = m_{prop}/(1 + MR) \quad (4.52)$$

Where:

- MR is propellant mixture ratio

Oxydizer/Fuel volume $[m^3]$ is given by eq. (4.53):

$$V_{ox/fuel} = 1.1 \cdot m_{ox/fuel} / \rho_{ox/fuel} \quad (4.53)$$

The value 1.1 is a safety factor.

Oxydizer/Fuel tank radius [m] and thickness are obtained by eqs. (4.54) and (4.55):

$$r_{tank_{ox/fuel}} = \sqrt[3]{\frac{3}{4} \cdot \frac{V_{ox/fuel}/_N}{\pi}} \quad (4.54)$$

$$t_{tank_{ox/fuel}} = \frac{sf \cdot P_{BOL} \cdot r_{tank_{ox/fuel}}}{2\sigma_y} \quad (4.55)$$

Where:

- N is tanks number
- Safety factor: $sf = 2$.

- Beginning of life pression for propellant tanks: $P_{BOL} = 2.4 \cdot 10^6 Pa$.
- Yield tension of material tank: σ_y.

Oxydizer/Fuel tank volume [m^3] and tank mass [kg] can be calculated by using eqs. (4.56) and (4.57):

$$V_{tank_{ox/fuel}} = \frac{4}{3} \cdot (r_{tank_{ox/fuel}} + t_{tank_{ox/fuel}})^3 - V_{ox/fuel} \quad (4.56)$$

$$\boldsymbol{m_{tank_{ox/fuel}}} = V_{tank_{ox/fuel}} \cdot \rho_{material} \quad (4.57)$$

Where:

- $\rho_{material}$ is tank material density

Pressurant mass for oxidizer and fuel
Blowdown system
It is assumed an adiabatic reversible transformation [35].
Volume of pressurant for oxidizer/fuel [m^3] is calculated with Poisson eq. (4.58):

$$V_{pres\ ox/fuel} = \frac{\left(\frac{P_{EOL}}{P_{BOL}}\right)^{\frac{1}{\gamma}} \cdot V_{ox/fuel}}{1 + \left(\frac{P_{EOL}}{P_{BOL}}\right)^{\frac{1}{\gamma}}} \quad (4.58)$$

Where:

- Beginning of life pression for pressurant tanks: $P_{BOL} = 2.07 \cdot 10^7 Pa$.
- End of life pression for pressurant tanks: $P_{EOL} = 689000\ Pa$.
- Biatomic gas: $\gamma_{N2} = 1.4$

Mass of pressuring for oxidizer/fuel [kg] eq. (4.59):

$$m_{pres\ ox/fuel} = \rho_{pres} \cdot V_{pres\ ox/fuel} \quad (4.59)$$

Where:

- ρ_{pres} is pressurant density

Total volume [m^3] and total mass [kg] of pressurant for oxidizer/fuel [m^3] are given by eqs. (4.60) and (4.61):

$$\boldsymbol{V_{tot\ pres}} = V_{pres\ ox} + V_{pres\ fuel} \quad (4.60)$$

$$\boldsymbol{m_{tot\,pres}} = m_{pres\,ox} + m_{pres\,fuel} \quad (4.61)$$

Cylindrical Tank for oxydizer and fuel

The cylindrical tank is considered with hemispherical domes.
Entering the length of the cylinder (L) as input, the tank radius [m] and thickness [m] of oxidizer/fuel are calculated by using eqs. (4.62) and (4.63):

$$r_{tank_{ox/fuel}} = \sqrt{\frac{V_{ox/fuel}}{L \cdot N \cdot \pi}} \quad (4.62)$$

$$t_{tank_{ox/fuel}} = \frac{1.5 \cdot P_{BOL} \cdot r_{tank_{ox/fuel}}}{\sigma_y} \quad (4.63)$$

Where:

- N is tanks number
- Beginning of life pression: $P_{BOL} = 2.4 \cdot 10^6 Pa$.
- Yield tension of material tank: σ_y.

Depending on the case and space availability within the lander, the user chooses to put the radius as an input as well.

Oxydizer/Fuel Tank mass [kg] is given by eq. (4.64):

$$m_{tank_{ox/fuel}} = N \cdot 2 \cdot \pi \cdot L \cdot r_{tank_{ox/fuel}} \cdot t_{tank_{ox/fuel}} \cdot \rho_{material} \quad (4.64)$$

Where:

- $\rho_{material}$ is tank material density

Spherical tank sizing of pressurant for oxidizer and fuel

Tank radius [m], tank thickness [m] and tank volume [m^3] of pressurant for oxydizer/fuel [m] can be calculated by using eqs. (4.65), (4.66) and (4.67):

$$r_{tank\,pres_{ox/fuel}} = \sqrt[3]{\frac{3}{4} \cdot \frac{V_{pres\,ox/fuel}/N}{\pi}} \quad (4.65)$$

$$t_{tank\,pres_{ox/fuel}} = \frac{sf \cdot P_{BOL} \cdot r_{tank\,pres_{ox/fuel}}}{2\sigma} \quad (4.66)$$

$$V_{tank\ pres_{ox/fuel}} = \frac{4}{3} \cdot (r_{tank\ pres\ ox/fuel} + t_{tank\ pres_{ox/fuel}})^3 - V_{pres\ ox/fuel} \quad (14.67)$$

Where:

- Yield tension of material tank: σ_y.
- Beginning of life pression for pressurant tanks: $P_{BOL} = 2.07 \cdot 10^7 Pa$.

Tank mass of pressurant for oxydizer/fuel [kg] is obtained by using eq. (4.68):

$$\boldsymbol{m_{tank\ pres_{ox/fuel}}} = V_{tank\ pres_{ox/fuel}} \cdot \rho_{material} \quad (4.68)$$

Tanks total mass of pressurant for oxydizer/fuel [kg] is given by sum of eq. (4.69):

$$m_{tot\ tank\ pres} = m_{tank\ pres_{ox}} + m_{tank\ pres_{fuel}} \quad (4.69)$$

Total Propulsion System mass [kg] is sum of all component mass previously calculated with margin of 5% as shown in eq. (4.70):

$$\boldsymbol{m_{tot}} = \left(m_{tank_{fuel}} + m_{tank_{ox}} + m_{tot\ tank\ pres} + m_{engine}\right) \cdot 1.05 \quad (4.70)$$

4.5 Structure

The task of the structure is to preserve the integrity of the pressurized module and the whole vehicle in general and protect the crew from any kind of load that may occur during ascent and descent.
The structure can be divided into three main parts:

- Primary structure, which is the backbone of the lander and provides structural strength and support for the other components. It represents the main protection of the pressurized module and is designed to withstand all forces and vibrations that may be present during all phases of the mission. It is usually constructed of aluminum alloys or composite materials.
- Secondary structure, which includes all the various components that contribute to the operation of the lander, such as solar panels (if included in the mission design), booms, and equipment racks attached directly to the primary structure.
- Tertiary structure, which includes all the smaller structures of the lander, such as scientific instruments, brackets, boxes or other

structures that change depending on the specific purpose of the mission [25].

In this thesis work, the lander considered is two-stage, and the main structure was assumed to be cylindrical, to simplify the calculations for the other subsystems as well.

4.5.1 Inputs & Outputs

INPUT

1. Dry mass from optimal staging [kg]
2. Payload mass [kg]

OUTPUT

1. Total Structure mass without HIAD: 10532 kg
2. Landing gear mass: 1705.2 kg
3. Mechanism mass: 1705.2 kg
4. Airlock mass: 400 kg
5. Airlock Volume: 2.5 m^3

4.5.2 Sizing Algorithm

Semi-empirical formulas were used to calculate the mass of the main components of the structure [25].

Total Structure mass without HIAD [kg] is given by using eq. (4.71):

$$\boldsymbol{m_{structure+TPS}} = 1.325 \cdot \left(\frac{dry\ mass}{1000}\right)^{2.683} + 5.651 \cdot 10^{-5} \cdot \left(\frac{dry\ mass + payload\ mass}{1000}\right)^{5.269} + 1390 \quad (4.71)$$

Where:

- The value of the dry mass is an input obtained from Optimal Staging algorithm.

Landing gear and mechanisms mass [kg] can be calculated by using eq. (4.72):

$$\boldsymbol{m_{landing\ gear}} = \boldsymbol{m_{mechanism}} = 0.08 \cdot \text{dry mass} \quad (4.72)$$

Airlock mass [kg] and volume are obtained with eqs. (4.73) and (4.74):

$$\boldsymbol{m_{airlock}} = 400\ kg \quad (4.73)$$

$$V_{airlock} = 2.5\ m^3 \quad (4.74)$$

4.6 Thermal Protection System

The Thermal Protection System is the first line of defense for the lander in protecting it against extreme heat sources. The TPS is especially critical during atmospheric reentry, as a lot of convective and radiative heat is generated by friction and violent impacts on surfaces. The structure and interior of the lander (especially the crew compartment) are protected, and it blocks, absorbs, and/or radiates the heat making sure that everything stays in the proper temperature ranges (especially the load-bearing structure). These systems are important contributors to the vehicle's dry mass, so it is important to understand how much heat they absorb per unit mass.
The main factors for selecting the TPS are time of heat exposure, speed of vehicle re-entry, and type of atmosphere.
External protection can make use of radiation, absorption or both to dissipate heat.

- Radiative systems reject about 80-90% of the heat through thermal radiation. They are the simplest and most reliable, but they withstand lower temperatures (up to 1400 °C) and are generally passive systems that do not involve changes in shape or mass.
- Absorption systems absorb heat through sinks, ablation or transpiration. They rely on absorption through phase changes, chemical reactions, temperature increases or cooling by transpiration/convection. They are typically very complex and heavy and often not reusable but can handle greater heat flows than radiative systems [25].

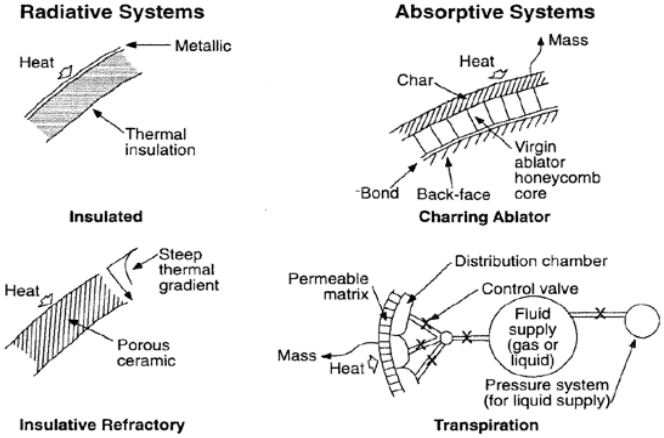

Figure 31: Concepts for Thermal Protection System

Although the Martian atmosphere is different and less dense than Earth's, it is dense enough to generate so much heat that the TPS on the manned lander is necessary.
A Hypersonic Inflatable Aerodynamic Decelerator (HIAD) for the descent, a type of technology that is relatively new and still under study, was chosen to size the lander's TPS.
During the EDL, once they contact the Martian atmosphere, the HIAD is inflated and expanded, which will protect the lander structure and slow it down. Upon reaching a certain descent velocity, the inflatable heat shield will be ejected, and retro-propulsion will be used to complete the landing.

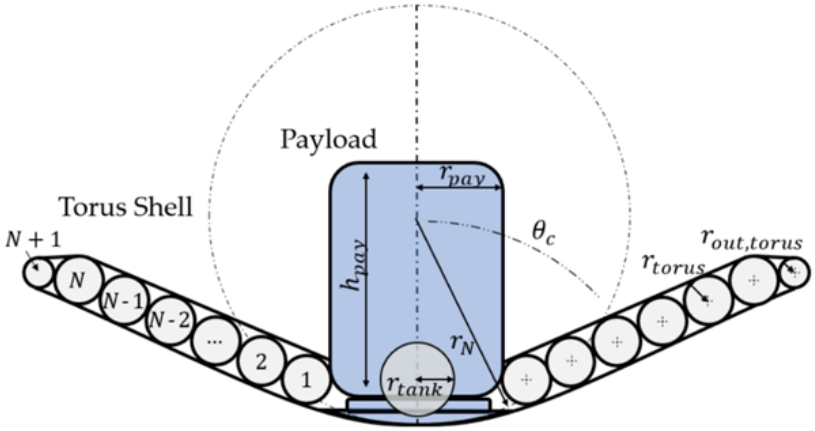

Figure 32: HIAD architecture

HIAD is composed of three main components.
The first major component is the center rigid heatshield, with modifications to accommodate the inflatable structures as well as attaching the second aeroshell. The aerocapture rigid nose does not need doors for the main engines. The second major component is the inflatable structure, the mass includes the torus liner, liner overlap, braid, braid overlap, coatings and adhesives, inflation and sense lines and other components. The third major component is the inflation system. The inflatable tori are covered with a non-ablative flexible TPS that protects the vehicle during aerocapture and entry [36].

4.6.1 Inputs & Outputs

INPUT

1. Rocket fairing [m]
2. Engines number [-]
3. Tori number [-]
4. Type of Inflation gas [-]

5. Heat shield material [-]
6. Tank material [-]
   ii) Yield tension [Pa]
   iii) Density $\left[\frac{kg}{m^3}\right]$

OUTPUT

1. Total TPS mass: 8431.54 kg
2. Inflate Volume: 102.08 m^3
3. Gas mass for HIAD: 123.85 kg
4. Gas tank mass: 90.29 kg
5. HIAD mass: 8217.4 kg

4.6.2 Sizing Algorithm

Fairing Starship

Radius of lander pressurized cylinder ($r_{pressurized}$) [6] can be used in eq. (4.75) to calculate the height [m] of pressurized cylinder:

$$h_{pressurized} = \frac{V_{pressurized}}{\pi \cdot (r^2_{pressurized})} \quad (4.75)$$

In case the geometrical characteristics of the engine are unknown, it's possible to estimate the length of the engine by using the eq. (4.76) in [37]. Engine length Turbopomp cycle [m]:

$$L_{engine} = 0.088 \cdot Thrust^{0.225} \cdot n_{engines}^{-0.4} \cdot \left(\frac{A_e}{A_t}\right)^{0.055} \quad (4.76)$$

Where:

- Area ratio: $\frac{A_e}{A_t} = 177$ [38]
- $n_{engines}$ is the number of engines
- $Thrust$ is total thrust required by lander

Lander total height [m] and width can be calculated by using eqs. (4.77) and (4.78):

$$h_{lander} = L_{engine} + h_{pressurized} \quad (4.77)$$

$$Width_{lander} = 2 \cdot r_{pressurized} + 2 \cdot r_{tank\,ps_{ox/fuel}} \quad (4.78)$$

From the height and width of the lander, you can see what the largest size is and from there you will decide the radius of the HIAD once it is inflated expanded (r_{infl}).

LANDER STRUCTURE

Shown in Figure 33 and Figure 34 is the very simplified architecture that has been assumed for the lander being designed in the following thesis.

The tanks are arranged all around the cabin containing the pressurized volume, while the engines are placed below. A landing gear has also been assumed so that the lander will land safely on the Martian surface.

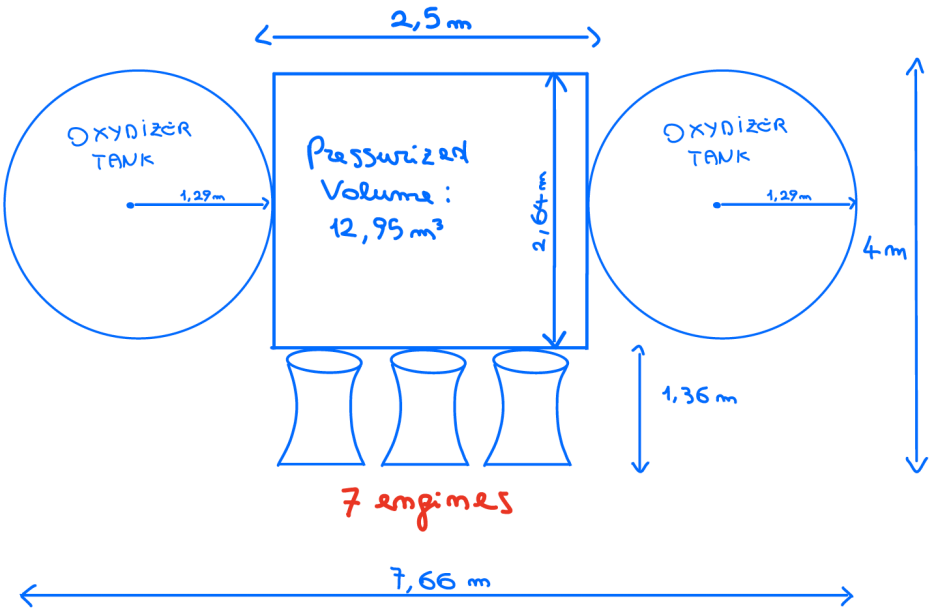

Figure 33: Lander structure from oxydizer tanks side

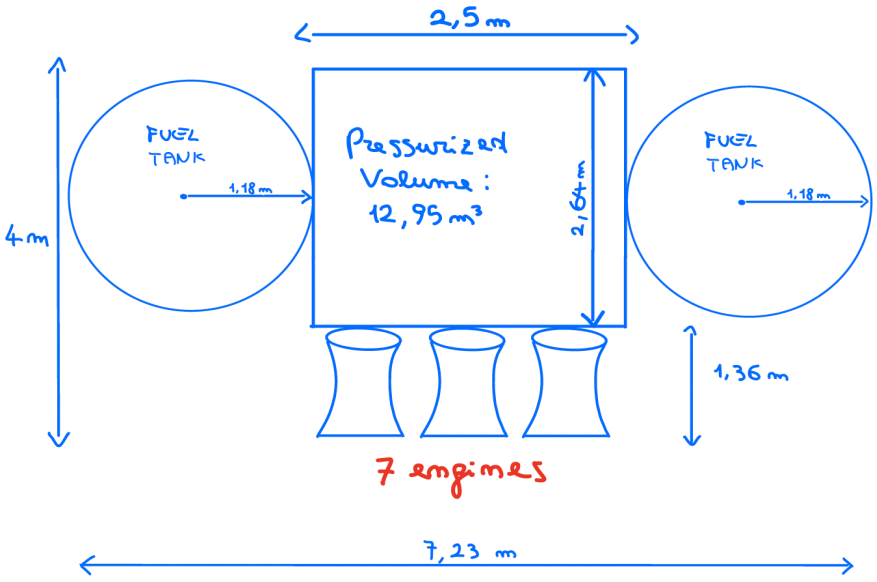

Figure 34: Lander structure from fuel tanks side

Gas Storage system

Gas inflation density $\left[\frac{kg}{m^3}\right]$ is given by using eq. (4.79):

$$\rho_{gas\ infl} = \frac{MM_{N2} \cdot p_{infl}}{R_{gas} \cdot T_{infl}} \quad (4.79)$$

Hypothesis of Scalable HIAD.

A very strong hypothesis, the scalability of the HIAD is a topic that is still being studied since the few HIADs designed were made ad hoc for various test missions [39].

Putting as input the total number of tori, from Figure 35 [39] can obtain the torus radius used in the eq (4.80).

All designs of Figure 35 have a 9 m diameter nose cone, 17.5 m major diameter and 70-degree cone angle.

Total # of tori	4	5	6	7	8	9	10	11	12	13	14	15
Torus radius (m)	0.39	0.31	0.26	0.22	0.19	0.17	0.15	0.14	0.13	0.12	0.11	0.10

Figure 35: Torus Radius in function of total number of tori

HIAD supposed as a cylinder

HIAD radius is the radius of base of the cylinder and torus diameter is the height that is calculated with eq. (4.80):

$$h_{infl} = r_{torus} = \frac{torus\ radius \cdot (r_{infl} \cdot 2)}{17.5} \quad (4.80)$$

Volume of HIAD [m^3] can be calculated by using eq. (4.81), while mass of inflatable gas is given by eq. (4.82):

$$\boldsymbol{V_{infl}} = \pi \cdot h_{infl} \cdot r_{infl} \quad (4.81)$$

$$\boldsymbol{m_{gas\ infl}} = \rho_{gas\ infl} \cdot V_{infl} \quad (4.82)$$

Where:

- Inflated pressure with margin: $p_{infl} = 44730\ Pa \cdot 1.25$.
- Inflated temperature: $T_{infl} = 213\ K$.
- Stored pressure of tank: $P_{tank_{infl}} = 4.8 \cdot 10^7 Pa$.

Spherical gas tank sizing
One tank for inflation gas
Tank volume of gas inflation [m^3] is calculated with eq. (4.83):

$$V_{gas\,tank} = m_{gas\,infl} / \rho_{gas\,tank} \quad (4.83)$$

Inflation gas tank radius [m] and thickness are calculated with eqs. (4.84) and (4.85):

$$r_{tank_{infl}} = \sqrt[3]{\frac{3}{4} \cdot \frac{V_{gas\,tank}/N}{\pi}} \quad (4.84)$$

$$t_{tank_{ox/fuel}} = \frac{sf \cdot P_{tank_{infl}} \cdot r_{tank_{infl}}}{2\sigma_y} \quad (4.85)$$

Where:

- Pressurant gas density N2 inside tank at 180 K and 48 Mpa: $\rho_{gas\,tank} = 674 \frac{kg}{m^3}$.
- Safety factor: $sf = 2$.
- Yield tension of material tank: σ_y.

Inflation gas tank mass [kg] is given by using eq. (4.86):

$$\boldsymbol{m_{tank_{infl}}} = 4 \cdot \pi \cdot \left(2 \cdot r_{tank_{infl}}\right)^2 \cdot t_{tank_{ox/fuel}} \cdot \rho_{material} \quad (4.86)$$

HIAD Mass
Always considering the scalability of the HIAD, proportion (4.87) is made with data from one HIAD present in [40].

$$\boldsymbol{m_{HIAD}} = \frac{10500 \cdot (r_{infl} \cdot 2)}{23} \quad (4.87)$$

4.7 Avionic System

The avionics system considered for the lander in this thesis consists of the Communication System and Command and Data Handling (C&DH). Usually in the avionics, AOCS is also included, but in this case it has been treated separately in a previous section so that it can be discussed in more detail.
The C&DH consists of an onboard computer, communication interfaces, memories, and other sensors, and allows crew members to interact with

data from all other subsystems. Specifically, it is tasked with processing data from sensors on board the lander in such a way as to activate/deactivate tools related to specific subsystems and manage the data (storage, storage and transmission). The Communication System is the other fundamental part of the avionics system and allows communication with the MOV and if possible, with the Earth. Thanks to this system, voice, video or scientific data can be transmitted and support of any kind can be given to the crew. Depending on the functions to be performed by the Communication System, the architecture can be more or less complex; this can be carried out through the use of antennas and other electronic instruments that help the transmission, stabilization and quality of the data transmitted [25] [41].

4.7.1 Inputs & Outputs

INPUT

1. Type of information: voice, video or data [-]
2. Orbit height [m]

OUTPUT

1. Data rate: bits/s or bps
2. Transmission delay: s
3. Propagation delay: 0.0017 s

4.7.2 Sizing Algorithm

The formulas used were taken from da [25] for very crude sizing, since it is difficult to make preliminary calculations for communications to and from Mars.

Data Rate [bits/s or bps] is calculated by using eq. (4.88):

$$\boldsymbol{R_d} = \left(\frac{message}{s}\right) \cdot \left(\frac{bytes}{message}\right) \cdot 8 \quad (4.88)$$

Data rate is proportional to the quantity of information per unit time transferred between the source and destination.

Transmission Delay [s] is calculated by using eq. (4.89):

$$\boldsymbol{t_{delay}} = \left(\frac{n_{bites} \cdot 8}{R_d}\right) \quad (4.89)$$

Time it takes to trasmit a block or packet of data.

Propagation Delay [s] is calculated by using eq. (4.90):

$$\boldsymbol{t_{prop}} = \left(\frac{distance\ from\ source\ to\ destination}{c}\right) \quad (4.90)$$

Amount of time the transmitted signal takes to travel between the source emitter and the destination receiver.

Where:

- Light speed: $c = 3 \cdot 10^8 m/s$

	Requirements Category			
Source	**Data Rate**	**Delay**	**Delay Jitter**	**BER**
Voice (e.g., crew-crew, space vehicle-EVA platform, and space vehicle-Earth comm)	Low (10s of kbps)	Low (<0.1 s)	Low (<0.01 s)	10^{-2} to 10^{-3}
Video (e.g., moving pictures, crew entertainment)	High (10s of Mbps)	Medium (0.5 to 1.5 s)	Medium (0.15 to 0.5 s)	10^{-5} to 10^{-7}
Data (e.g., experimental data, software uploads)	Variable (kbps through Mbps)	Variable (up to minutes)	Variable (up to seconds)	10^{-5} to 10^{-7} (and higher)

Figure 36: Typical requirements of Sources of Voice, Video and Data information [25]

4.8 Thermal Control System

The Thermal Control System is the subsystem that is responsible for making a heat balance between incoming and outgoing heat to ensure a comfortable temperature for the crew inside the cabin and ensure that the components remain within a precise and stringent temperature range.
The main functions of TCS are:

1. Ensure a specific temperature range for crew members so that their stay inside the lander is comfortable.
2. Avoiding excessive temperature gradients, i.e., preventing parts of the structure from having temperatures that are too different from others, on pain of structural deformation, which can cause structural damage and problems to other subsystems of the lander.

3. Ensure appropriate temperature ranges for all components of the various subsystems. The ranges to be observed are as follows:
   i) Operational, which is the ideal operating range;
   ii) Survival, i.e., the range outside which there is permanent damage to the components.

The two worst cases in which it is necessary to design and size the lander TCS are:

- Hot case which represents a condition in which the lander is subjected to higher thermal stress and maximum power is dissipated from all subsystems. In this case, the hot case occurs in ascent when the lander is under the greatest thermal stress and the power dissipation is max.
- Cold case, a condition in which the lander dissipates the least power and is placed in an extremely cold environment. This case occurs when the lander is on the Martian surface at night and in hibernation mode (low power consumption mode on Mars surface without crew inside).

Thermal control can be done passively, actively, or a combination of the two. Passive techniques make use of materials, coatings or surfaces to maintain temperature in the desired ranges, all without active use of power. Active techniques maintain the temperature in the set ranges by appropriate means, such as heat exchangers, heat pipes, radiators, etc., all of which involve active intervention of any kind.

As for the lander being designed, for the hot case fixed radiators are used to dissipate heat loads, while for the cold case for heating the crew cabin heaters are used, hence the use of a mix of active and passive thermal control [25].

4.8.1 Inputs & Outputs

INPUT

1. Max and min Mars temperature [K]
2. Lander measures (height, width) [m]
3. Coating material [-]
   i) Absorbtivity [-]
   ii) Emissivity [-]
4. Type of radiator [-]
   i) Fixed [-]
   ii) Deployable [-]
5. Crew number [-]

OUTPUT

1. Infrared max flux on Mars: 330.8 $\frac{W}{m^2}$
2. Infrared min flux on Mars: 3.32 $\frac{W}{m^2}$

HOT CASE

1. Emitted flux coating: 5586.7 W
2. Heat to reject in sunlight: 17865 W
3. Radiators surface: 55.69 m^2
4. Radiators mass: 295.13 kg
5. Radiators Volume: 1.1137 m^3
6. Radiators Power: negligible

COLD CASE

1. Heat to give to the lander: 2969.6 W
2. Heaters mass: 2.08 kg

4.8.2 Sizing Algorithm

Max/min flux on Mars $\left[\frac{W}{m^2}\right]$ is given by eq. (4.91):

$$\boldsymbol{Max/Min_{ir\ flux}} = Stef_{Bolz} \cdot em_{Mars} \cdot \left(T^4_{max/min_{surf}} - T^4_{sink\ max/min}\right) \quad (4.91)$$

Where:

- Max sink temperature: $T_{sink\ max} = 150\ K$.
- Min sink temperature: $T_{sink\ min} = 133\ K$.
- Mars emissivity: $em_{Mars} = 0.85$
- $Stef_{Bolz} = 5.67 \cdot 10^{-8}\ \frac{W^2}{\frac{m^2}{K^4}}$.

HOT CASE

Cross section of the lander cabin supposed as a cylinder [m^2], so it can be calculated by using eq. (4.92):

$$S_{frontal} = 2 \cdot h_{lander} \cdot r_{lander} \quad (4.92)$$

Where:

- h_{lander} is the height of lander
- r_{lander} is the radius of lander

Sun heat [W], Albedo heat from Mars [W] and Infrared heat from Sun [W] are obtained by using eqs. (4.93), (4.94) and (4.95):

$$Q_{sun} = S_{frontal} \cdot const_{Sun} \quad (4.93)$$

$$Q_{albedo} = Q_{sun} \cdot mars_{albedo} \quad (4.94)$$

$$IR_{sun} = S_{frontal} \cdot Max_{ir\,flux} \cdot \left(\frac{r_{Mars}}{r_{mars}+h_{orbit}}\right)^2 \quad (4.95)$$

Where:

- Solar flux on Mars: $const_{Sun} = 590\ \frac{W}{m^2}$.
- $mars_{albedo} = 0.25$. Albedo is a measure of Mars' reflexivity

Total lander surface (lander supposed as a cylinder) [m^2] can be calculated by using eq. (4.96):

$$S_{tot\,lander} = 2 \cdot \pi \cdot h_{lander} \cdot r_{lander} + 2 \cdot \pi \cdot {r_{lander}}^2 \quad (4.96)$$

Emitted flux coating heat [W] is given by eq. (4.97):

$$\boldsymbol{Q_{em_{coat}}} = Stef_{Bolz} \cdot em_{coating} \cdot S_{tot\,lander} \cdot T_{\max op}^4 \quad (4.97)$$

Where:

- Max operating temperature: $T_{\max op} = 313\ K$.
- $em_{coating}$ is the emissivity of coating surface

Total heat to manage [W] can be calculated by using eq. (4.98), while Absorbed heat by lander [W] is given by eq. (4.99):

$$Q_{tot} = Q_{sun} + Q_{albedo} + IR_{sun} \quad (4.98)$$

$$Q_{absorbed} = Q_{tot} \cdot absorbivity_{coating} \quad (4.99)$$

Where:

- $absorbivity_{coating}$ is the absorbivity of coating surfaces

For the calculation of the peak power required by the lander, a semi empirical formula was used [25], since the level of detail was not sufficient to estimate

the power of each subsystem and obtain the total peak power that the lander requires in its highest demand phase.

Average power [W] and peak power of lander subsystem [W] are obtained by eqs. (4.100) and (4.101):

$$P_{avg} = 1000\ W + 500W \cdot n_{crew} \quad (4.100)$$

$$P_{tot} = P_{avg} \cdot 1.75 \quad (4.101)$$

Heat budget to reject by the system active in sunlight [W] is calculated with eq. (4.102):

$$\boldsymbol{Q_{rejected}} = P_{tot} + Q_{absorbed} - Q_{em_{coat}} \quad (4.102)$$

Radiators surface [m^2], radiators mass [kg] and radiators volume [m^3] are obtained by using eqs. (4.103), (4.104) and (4.105):

$$\boldsymbol{S_{radiators}} = \frac{Q_{rejected}}{em_{radiator} \cdot Stef_{Bolz} \cdot T_{radiator}^4} \quad (4.103)$$

$$\boldsymbol{rad_{mass}} = 5.3 \cdot S_{radiators} \quad (4.104)$$

$$\boldsymbol{rad_{vol}} = 0.02 \cdot S_{radiators} \quad (4.105)$$

Where:

- Radiators temperature: $T_{radiator} = 290\ K$.
- $em_{coating}$ is the emissivity of radiator

COLD CASE

Radiations from sun for the cold case [W] and Emitted flux coating heat [W] are calculated by using eqs. (4.106) and (4.107):

$$Q_{external_{cold}} = S_{frontal} \cdot Min_{ir\ flux} \cdot \left(\frac{r_{Mars}}{r_{mars} + h_{orbit}}\right)^2 \quad (4.106)$$

$$Q_{em_{coat}} = Stef_{Bolz} \cdot em_{Mars} \cdot (T_{min} - 10°)^4 \quad (4.107)$$

Where:

- r_{mars} is Mars radius
- h_{orbit} is circular height orbit

- Minimum operative temperature for considered system $T_{min} = 273\ K$.

The heat to give to the lander [W] is given by subtraction in eq. (4.108):

$$\boldsymbol{Q_{heater_{cold}}} = Q_{em_{coat}} - Q_{external_{cold}} \quad (4.108)$$

Heaters mass [kg] [25] is given by eq. (4.109):

$$\boldsymbol{heaters_{mass}} = 0.7 \cdot \left(\frac{Q_{heater_{cold}}}{1000}\right) \quad (4.109)$$

4.9 Electrical Power System

The Electrical Power System is critical for the support of crew life inside the lander habitable module and for powering the various subsystems that require electrical power. The EPS must necessarily be safe, reliable and a regular power source.
The main functions of this subsystem are:

- Provide electrical power;
- Store it;
- Distributing it;
- Regulating and conditioning on the same.

There are also ancillary functions:

- Exchanging information with other subsystems, interfacing mainly with the C&DH, which receives information and sends commands;
- Monitor its health status and operations;
- Protect itself and other subsystems from malfunctions [42].

For the EPS to perform these functions, it can be divided into three additional subsystems:

1. The primary power subsystem, which is the system that generates electrical power from the raw source, stores this energy and distributes it to the main buses.
2. Power management and distribution subsystem, which is responsible for taking power from the main buses and distributing it to the end users.
3. Storage subsystem, which oversees storing this energy and using it at the most appropriate time [25].

The three main sources of electricity are: solar, chemical and nuclear. The former has been ruled out a priori because sandstorms may occur on the

surface of Mars, which could partially obscure the Sun and thus render power generation tools, such as solar panels, almost completely useless.
The following paragraphs will explore various possibilities that the user can select for power generation, distribution, and storage.

4.9.1 Inputs & Outputs

INPUT

Energy storage

1. Power budget of all subsystems [W]
2. Type of battery [-]
   i) $Energy_{battery}$ $[Wh]$
   ii) Battery energy density
3. Type of fuel cell
4. Number of tanks N [-]
5. Tanks material [-]
   i) Yield tension [Pa]
   ii) Density $\left[\frac{kg}{m^3}\right]$

OUTPUT

ENERGY STORAGE

Battery

1. Battery capacity: 22105 Wh^2
2. Battery mass: 157.9 kg

Fuel cell

1. Total Fuel Cell mass: 797.43 kg
2. H2 mass: 14.97 kg
3. O2 mass: 118.14 kg
4. H2 tank mass: 498.47 kg
5. O2 tank mass: 127.5 kg
6. H2O tank mass: 0.37 kg

ENERGY GENERATION

1. MMRTG mass: 2304 kg
2. GPHS RTG mass: 1102 kg
3. DPRS mass: 3000 kg

ENERGY DISTRIBUTION

Cable mass: 540 kg

4.9.2 Sizing Algorithm

Energy storage - Batteries

A battery is a device for storing electrical energy by a chemical process that it subsequently releases in a controlled manner in the form of direct current. The basic requirement of any battery is to provide the required power, at the desired voltage, and for as long as it is set. This requirement must be pursued by trying to minimize the size, volume, and cost of the battery pack. In addition, it must be able to mechanically withstand the shocks and vibrations it will encounter, dissipate the heat generated while maintaining uniform temperature, and minimize voltage drop.

Total time for using battery [s] is given by eq. (4.110):

$$t_{total} = n_{days} \cdot 24 \cdot 3600 \quad (4.110)$$

Where:

- n_{days} is the time in which batteries are used

Battery capacity [Wh^2] and batteries number can be calculated by using eqs. (4.111) and (4.112):

$$\boldsymbol{C_{battery}} = \frac{P_{tot} \cdot t_{total}}{DOD \cdot \eta} \quad (4.111)$$

$$N_{battery} = \frac{C_{battery}}{Energy_{battery}} \quad (4.112)$$

Where:

- Depht of discarge of battery: DOD
- Battery efficiency: $\eta = 0.95$.
- P_{tot} is the power budget of lander
- $Energy_{battery}$ $[Wh]$

Batteries mass [kg] is obtained by using eq. (4.113):

$$\boldsymbol{m_{battery}} = \frac{C_{battery}}{\rho_{energy_{battery}}} \quad (4.113)$$

Where:

- Battery energy density: $\rho_{energy_{battery}}$

Energy storage – Fuel Cell

Fuel cells are devices that generate electricity through the conversion of chemical energy resulting from the oxidation reaction.
They are classified according to the electrolyte they use, and this determines the type of chemical reactions that take place, the type of catalyst needed, the operating temperature range, and the fuel required.
The fuel cell most widely used in space and considered in this study is the hydrogen-oxygen fuel cell, which through a reaction that is the reverse of electrolysis forms water that can be drunk by crew members.

O2 and H2 mass

Oxygen and Hydrogen flow $\left[\frac{kg}{s}\right]$ for a fuel cell system with a given power $\left[\frac{kg}{s}\right]$ can be calculated by using eqs. (4.114) and (4.115):

$$O_{2\,prod} = 8.29 \cdot 10^{-8} \cdot \left(\frac{P_{tot}}{V_c}\right) \quad (4.114)$$

$$H_{2\,prod} = 1.05 \cdot 10^{-8} \cdot \left(\frac{P_{tot}}{V_c}\right) \quad (4.115)$$

Where:

- Average cell voltage: $V_c = 0.65$ V.

Total Oxygen and Hydrogen required [kg] is given by eqs. (4.116) and (4.117):

$$\boldsymbol{O_{2\,tot}} = O_{2\,prod} \cdot 60 \cdot 60 \cdot 24 \cdot n_{days} \quad (4.116)$$

$$\boldsymbol{H_{2\,tot}} = H_{2\,prod} \cdot 60 \cdot 60 \cdot 24 \cdot n_{days} \quad (4.117)$$

Total Oxygen and Hydrogen volume $[m^3]$ can be obtained by using eqs. (4.118) and (4.119):

$$V_{LO2} = O_{2\,tot} / \rho_{LO2} \quad (4.118)$$

$$V_{LH2} = H_{2\,tot} / \rho_{LH2} \quad (4.119)$$

The formulas for calculating the required amount of hydrogen and oxygen were taken here [43].

LO2, LH2 and water spherical tank sizing

H2O/LO2/LH2 tank radius [m] and thickness [m] cab be obtained by using eqs. (4.120) and (4.121):

$$r_{tank_{H2O/LO2/LH2}} = \sqrt[3]{\frac{3}{4} \cdot \frac{V_{H2O/LO2/LH2}/_N}{\pi}} \quad (4.120)$$

$$t_{tank_{H2O/LO2/N2}} = \frac{sf \cdot P_{tank_{H2O/L02/LH2}} \cdot r_{tank_{H2O/LO2/LH2}}}{2\sigma_y} \quad (4.121)$$

Where:

- Yield tension of material tank: σ_y.
- Safety factor: $sf = 2$.
- Pression of liquid O2 tanks: $P_{tank\,LO2} = 4 \cdot 10^7 Pa$. [44]
- Pression of liquid H2 tanks: $P_{tank\,LH2} = 7 \cdot 10^7 Pa$.
- Pression of liquid H2O tanks: $P_{tank\,H2O} = 2 \cdot 10^5 Pa$.

H2O/LO2/LH2 tank volume [m^3] can be calculated by using eq. (4.122), while H2O/LO2/LH2 tank mass [kg] is given by eq. (4.123):

$$V_{tank_{H2O/LO2/LH2}} = \frac{4}{3} \cdot (r_{tankh2o/_{LO2/LH2}} + t_{tank_{h2o/LO2/LH2}})^3 - V_{H2O/LO2/LH2} \quad (4.122)$$

$$\boldsymbol{m_{tank_{H2O/LO2/LH2}}} = V_{tank_{H2O/L02/LH2}} \cdot \rho_{material} \quad (4.123)$$

Total Fuel Cell mass [kg] is sum of all component mass previously calculated with margin of 5% as shown in eq. (4.124):

$$\boldsymbol{m_{tot}} = \left(m_{tank_{H2O}} + m_{tank_{LH2}} + m_{tank_{LO2}} + O_{2\,tot} + H_{2\,tot}\right) \cdot 1.05 \quad (4.124)$$

Energy generation – MMRTG
(Multi-Mission Radioisotope Thermoelectric Generator)

Regarding the generation of electricity by nuclear power, the MMRTG can be used. This instrument employs a thermoelectric conversion method to generate power from the heat created by the natural decay of plutonium-238. For missions that need to operate in distant and difficult areas for an extended period, the MMRTG offers a reliable and long-lasting power supply [42]. It is used as a power generation tool on the Curiosity and Perseverance rovers.

- Power BOL: 110 W
- Mass: 48 kg

- Thermal power: $\sim 2000\ W$

5250 W of Power Budget:
- # MMRTG: 48
- Total mass: 2304 kg
- Total heat to manage: $\sim 96\ kW$

Energy generation – DRPS
(Dynamic Radioisotope Power system)
To conclude, the last power generation instrument using nuclear energy that is analyzed is the DRPS. It is an instrument still under development by NASA (TRL 5) and is like the MMRTG, in fact it too employs a radioisotope heat source, but it has a motor that converts thermal energy into mechanical motion, which powers an electric generator. Thus, the DRPS seeks to take advantage of moving parts to increase the efficiency of this energy conversion up to three or four times that of the previously mentioned MMRTG [45].

- Power: 200-500 W
- Mass: 200 kg

Dato che il power budget considerato è di 5250 W:
- # DPRS: 15
- Total mass (350 W): 3000 kg

The performances considered for the MMRTG and DPRS, were taken in the Figure 37 [46]:

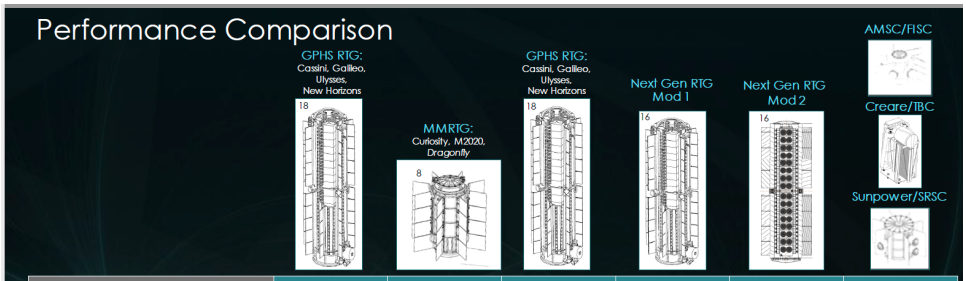

Parameter	GPHS-RTG	MMRTG	Next Gen Mod 0	Next Gen Mod 1	Next Gen Mod 2	DRPS
P_{BOL} (W_e)	291	110	293	245	400	300 to 400
Mass (kg)	58	44	56	56	56	100 to 200
Q_{BOL} (W_{th})	4410	2000	4500	4000	4000	1500
P_{EODL}, $P=P_0*e^{-t}$ (W_e)	N/A	63	208	177	290	241 to 321
Maximum Average Annual Power Degradation, r (%/yr)	1.54	3.8	1.9	1.9	1.9	1.3
Fueled Storage Life, t (yrs)	2	3	3	3	3	3
Flight Design Life, t (yrs)	16	14	16	14	14	14
Design Life, t (yrs)	18	17	18	17	17	17
Allowable Flight Voltage Envelope (V)	22-34	22-34	22-34	22-36	22-36	22 to 36
Planetary Atmospheres (Y/N)	N	Y	N	N	N	Y
Estimated Launch Date Availability	N/A	Now	2026	2029	2034	2030

Figure 37: Performance comparison from nuclear electric generation devices

The other technologies in the Figure 37 were not considered because they were either out of use such as GPHS RTGs as they were used for missions decades ago or still too immature such as Next Gen Mod 1 and 2.

Energy distribution - cable

Using data from a study conducted [47] it is assumed that there is a power plant on the surface of Mars that produces electricity and cables that will have to be connected to the lander once it lands in such a way as to supply it with this energy. The cables that will be used are not part of the lander and therefore have the advantage of not weighing it down and are cables that are assumed to operate with a voltage of 1000V DC. The lander landing will have to be made on a base that is approximately 1 km from the power plant. The user will have to select as input the peak power required by the lander and as output will get the mass of the cables that will distribute the power from the power plant to the lander through the graph in Figure 38 [47].

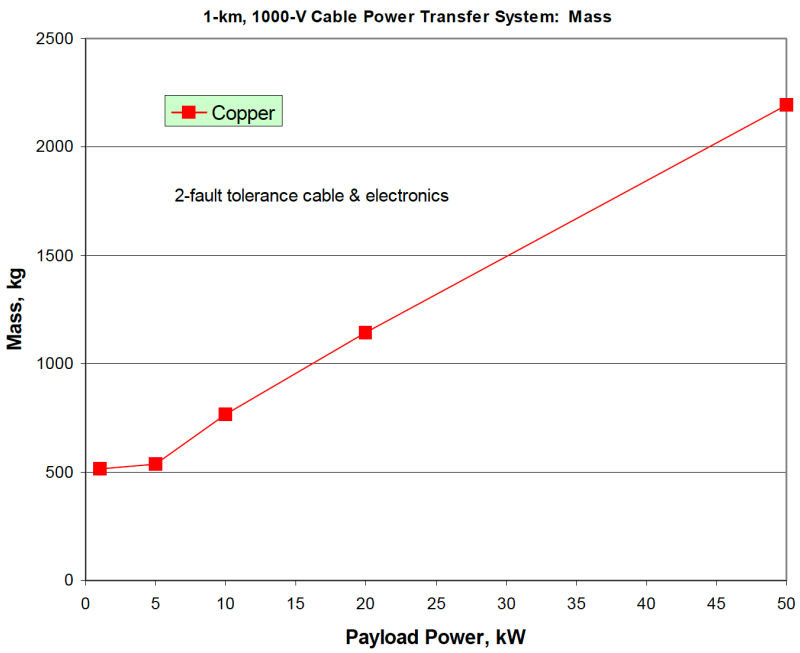

Figure 38: Mass vervus payload power level

Choise to be selected by the user

Three possible solutions have been hypothesized for the user to choose to realize the EPS of the MAV.

- **FIRST CHOICE:** batteries sized for ascent and descent + cables on the Martian surface (lander ibernation mode) -> low power consumption mode on Mars surface without crew inside, to keep the system operative and to survive for the long stay of humans on Mars.

- **SECOND CHOICE:** fuel cell for the entire duration of ascent, descent and 2 days on the surface
- **THIRD CHOICE:** DPRS or MMRTG

4.10 New subsystems percentages on ascent dry mass

Dry mass: 17921 kg

- **Propulsion system:** 29.471% dry mass -> 5281.52 kg
- **TCS:** 1.659% dry mass -> 297.21 kg
- **Structure + TPS (without HIAD):** 58.769% dry mass -> 10532 kg
- **EPS (fuel cell):** 4.45% dry mass -> 797.43 kg
- **ECLSS:** 3.983% dry mass -> 713.81 kg
- **Avionic (TT&C and C&DH):** 0.953% dry mass -> 170.9 kg
- **AOCS:** 0.715% dry mass -> 128.13 kg

After the first iteration of sizing was finished, considering the outputs obtained through the choice of ad hoc inputs, the total masses of each subsystem were calculated and the percentage in mass of each subsystem relative to the dry mass of the lander was calculated.
This made it possible to update the percentages obtained at the end of the study done in section *3.2 First Design Methodology & Starting Point for Subsystem Design.*
Also, note how the dry mass value obtained at the end of this first iteration is lower than the 21315 kg obtained as output from the Optimal Staging algorithm. The subsystems that impact the most on the dry mass of the lander are the Propulsion System and Structure, while the least influential ones are mostly the electronic systems such as Avionic and AOCS.
The sizing that was done in this chapter has a level of detail that is not very high, so the percentages obtained are to be taken with a grain of salt and will be updated with future iterations and as the calculations are refined.

4.11 Architecture Change

This section will discuss other lander configurations that enable EDL other than the one assumed in the previous paragraphs. In addition to the HIAD, used as the TPS for the descent phase of the lander being designed, two other architectures will be analyzed: the ADEPT (Adaptable Deployable Entry Placement Technology) and the Capsule.
We will focus mainly on the TPS, since it is the subsystem of greatest interest and the one most affected by this change that we want to study.

4.11.1 Assumption

To make the comparison between the various architectures, the following assumptions will be made:

- Subsystems like power, avionics, and payload (cargo), were assumed to be identical in all configurations.
- All vehicles assumed the same core lander structure for the vertical packaging arrangement.
- The avionics sub-system covers the communications systems, command and data handling systems, and the guidance, navigation, and control systems
- Other subsystems, like the aeroshell structures and thermal protection system, as well as the propellant volume and tank sizing, were unique to each configuration.
- All configurations consist of a circular descent module that houses the propellant tanks, engines, and all other subsystems protected by a heat shield [48].

4.11.2 ADEPT

Adaptable deployable entry placement technology

The ADEPT is a rigid deployable, unlike the HIAD which is an inflatable deployable.
The main components of the ADEPT are: the rigid nose, the deployable decelerator, ribs and struts, the deployment system and the integration with the structure of the lander.

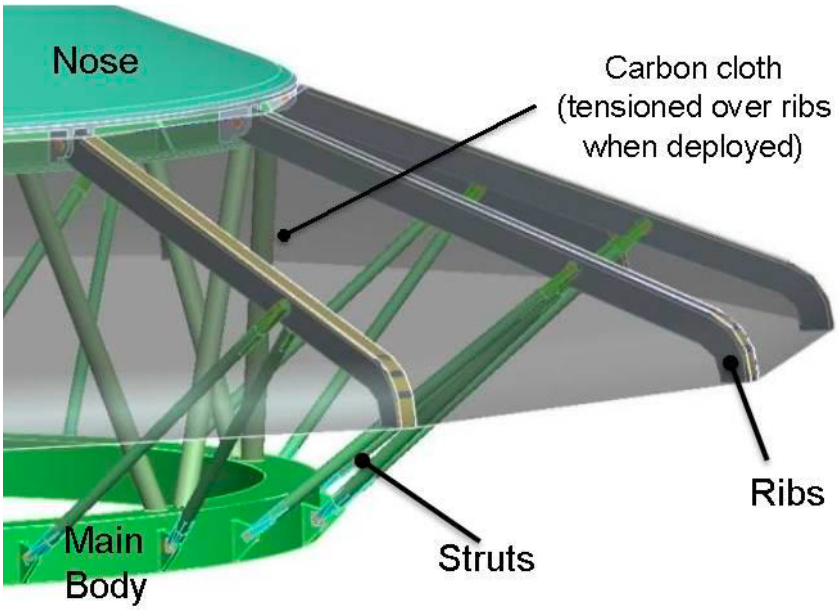

Figure 39: ADEPT components, deployment system

The nominal structural arrangement is depicted in the Figure 39.
The key technological element of the ADEPT is the multilayer flexible carbon fabric that forms a semi-rigid membrane when pretensioned by the deployment of the support ribs.
The lower layers of the fabric transfer aerodynamic load to the support structure, while the upper layers manage thermal energy.
The rigid nose is composed of a conventional material and is a carrier structure that includes compression pads and upper stage adapter, as well as a seal between rigid nose and the deployable carbon fabric
The main body is composed of structural rings to react to loads from the ribs and struts and to interface with the lander [49].
The ribs are longer on one side than on another so that an asymmetrical shape is achieved to make the desired lift-to-drag-ratio. The ribs are assumed to be made from graphite composite material and the struts from titanium.

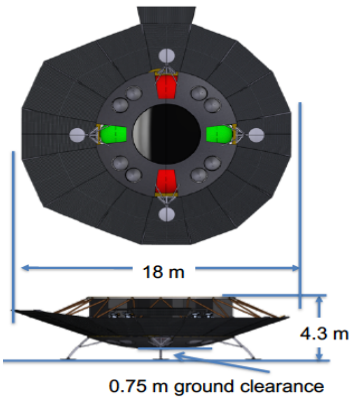

Figure 40: ADEPT bottom and side with dimensions

The structure also includes engine nozzle and landing leg exit doors. Since no elements can be jettisoned, it is assumed that the doors slide open during entry after peaking dynamic pressure [50].
This study shows that the percentage of TPS on dry mass weight is 40.5%.

4.11.3 Capsule

This type of architecture has a shape adapted for Mars entry capsules. Also, unlike HIAD and ADEPT, there is no deployable element in this configuration, but a design with a rigid heat shield was assumed.

Figure 41: Capsule bottom and side with dimensions

The rigid heat shield consists of two parts:

- Backscell, which corresponds to the top of the Capsule and not in direct contact with the heat generated by friction between the vehicle and the Martian atmosphere;
- Heatshield, which corresponds to the lower part of the lander, where there are ports for the engines and the 4 legs of the landing gear, and is the part of the lander where the most heat is generated.

The backshell is assumed to consist of a layer of Aluminum alloy 2024 covered by room temperature vulcanizing (RTV) insulation and Super Lightweight Ablator (SLA-5610).
The heatshield material consists of a layer of aluminum honeycomb or a sandwich layer with a carbon fiber-reinforced polymer (CFRP) composite laminate system face-sheet called IM7 and a layer of RTV with Phenolic-Impregnated Carbon Ablator (PICA) ablative TPS [24]. The TPS layers are represented in Figure 42.

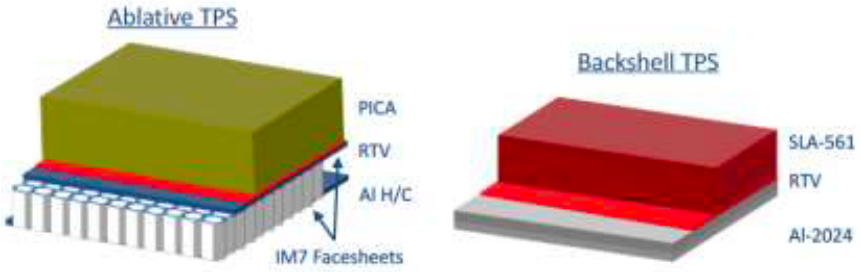

Figure 42: Heatshield and backshell TPS

This study shows that the percentage of TPS on dry mass weight is 35.5%.

Chapter 5

Validation

In this chapter an attempt will be made to validate all the algorithms used in Subsystem Design for sizing the various subsystems from which the designed lander is composed. Tables will be drawn up for each subsystem in which there will be:

- the values calculated with the algorithms used in this thesis work;
- the values present in the reference used to validate the algorithm;
- the relative errors in percent calculated with eq. (5.1);
- the unit of measurement used for those values.

$$Error\ [\%] = \frac{|Calculated\ value - Reference\ value|}{Reference\ value} \cdot 100 \quad (5.1)$$

Each table will contain the total mass of the individual subsystem and the mass, volume, and if necessary, the power of the individual components considered in the previous chapter. Validation is lacking for some components, as it is difficult to find specific data in the literature.

5.1 Attitude & Orbit Control System

To validate AOCS design routine, the project data of [51] are used. Table 10 shows the comparison between [51] results and methodology final data of this thesis.

NUMERICAL INPUT

- Propellant type: MMH/MON25
  - Isp: 343 s
  - Density MON 25: 1400 $\frac{kg}{m^3}$
  - Density MMH: 800 $\frac{kg}{m^3}$
- Delta V for aocs manouvers: 52.65 m/s
- Mixture ratio: 2.4
- Tank material: DURAL 2024

    - Yield tension: 300 MPa
    - Density: 2700 $\frac{kg}{m^3}$
- Fuel tank number: 1
- Fuel oxydizer number: 1

AOCS	Thesis	[51]	Error [%]	Unit
AOCS TOTAL MASS	71.02	73.37	3.2	[kg]
Propellant mass	67.33	68.85	-2.21	[kg]
Tank mass (oxydizer + fuel)	3.69	4.52	-18.36	[kg]
Total propellant volume	0.0565	0.0577	-2.15	$[m^3]$

Table 10: AOCS validation values

The only major error that has been calculated is the one concerning the total tank mass, but on the total subsystem mass it affects relatively little.

5.2 Enviromental Control & Life Support System

To validate ECLSS design routine, the project data of [52] are used. Table 11 shows the comparison between [52] results and methodology final data of this thesis.

NUMERICAL INPUT

- Number of crew members: 4
- Residence time inside the lander: 3 days
- Type of atmosphere: 30 % Oxygen and 70% Nitrogen

ECLSS	Thesis	[52]	Error [%]	Unit
ECLSS TOTAL MASS	721.23	635.3	13.52	[kg]
Habitable volume	11.14	7.93	40.48	$[m^3]$

Total mass oxygen + nitrogen	26.26	32	-17.93	[kg]
Tanks total mass	15.62	12.3	27	[kg]
Total mass component	679.35	591	14.95	[kg]
Total volume components	1.8	-	-	$[m^3]$
Total power components	3113	3766	-17.34	[W]

Table 11: ECLSS validation values

5.3 Propulsion System

To validate Propulsion System design routine, the project data of [53][54] are used. Table 12 shows the comparison between [53][54] results and methodology final data of this thesis.

NUMERICAL INPUT

- Engines number: 1
- Delta V: 2220 m/s
- Propellant type: MMH/N2O4
  - Isp: 310 s
  - Fuel Density: 903 $\frac{kg}{m^3}$
  - Oxydizer Density: 1450 $\frac{kg}{m^3}$
- Mixture ratio: 1.6
- Fuel tank number: 1
- Oxydizer tank number: 1
- Tanks number for pressurant: 2
- Tanks material: Alclad 24 ST
  - Yield tension: 345 MPa
  - Density: 2700 $\frac{kg}{m^3}$
- Pressurant type: Helium
  - Density: 28.33 $\frac{kg}{m^3}$

Propulsion System	Thesis	[53]-[54]	Error [%]	Unit
PS TOTAL MASS	2679.18	2518	6.4	[kg]
Total mass engine	18.86	63.96	-70.51	[kg]
Propellant mass	2575.1	2371.4	8.59	[kg]
Propellant tank mass	71.53	70.2	1.9	[kg]
Total pressurant mass	6.69	5.9	13.39	[kg]
Total pressurant tank mass	7	6.53	7.2	[kg]

Table 12: Propulsion System validation values

The Propulsion System, along with Structure, is the system that has the greatest influence on the total weight of the lander. Except for the total mass of the engine, which has little influence on the total mass of this subsystem, the percentage errors obtained are relatively low.

5.4 Structure

To validate Structure design routine, the project data of [52] are used. Table 13 shows the comparison between [52] results and methodology final data of this thesis.

NUMERICAL INPUT

- Dry mass: 12141 kg
- Payload mass: 455 kg

Structure	Thesis	[52]	Error [%]	Unit
STRUCTURE TOTAL MASS WITHOUT HIAD	3151.3	2934	7.41	[kg]
Landing gear mass	979.28	788	24.27	[kg]

Mechanism mass	979.28	-	-	[kg]

Table 13: Structure validation values

The total mass of Structure has a relatively low percentage error. The weight of the landing gear, on the other hand, was calculated very crudely by considering a percentage to the mass of the structure, which is why it differs from the weight calculated in [52].

5.5 Thermal Protection System

To validate TPS design routine, the project data of [20] are used. Table 14 shows the comparison between [20] results and methodology final data of this thesis.

NUMERICAL INPUT

- Rocket fairing: 16 m
- Tori number: 4
- Type of Inflation gas: Nitrogen
  - Density: 674 $\frac{kg}{m^3}$
- Tank material: Kevlar 49
  - Yield tension: 2970 MPa
  - Density: 1440 $\frac{kg}{m^3}$

TPS	Thesis	[20]	Error [%]	Unit
TPS TOTAL MASS	2224.46	2014	10.45	[kg]
Inflate Volume	71.7	-	-	$[m^3]$
Gas mass for HIAD	154.5	137	12.77	[kg]
Gas tank mass	53.06	57	-6.92	[kg]
HIAD mass	2017.4	1820	10.84	[kg]

Table 14: TPS validation values

In general, the results obtained with the algorithm used in this thesis work differ relatively little from the reference used. The only output not available is that of inflate volume.

5.6 Thermal Control System

To validate TCS design routine, the project data of [55] are used. Table 15 shows the comparison between [55] results and methodology final data of this thesis.

NUMERICAL INPUT

- Max Moon temperature: 400 K
- Lander measures:
  - Height: 9.9 m
  - Widht: 7.6 m
- Coating material:
  - Absorbtivity: 0.545
  - Emissivity 0.706
- Type of radiator: Fixed
- Crew number: 4

TCS	Thesis	[55]	Error [%]	Unit
TCS TOTAL MASS	-	-	-	[kg]
Heat to reject in sunlight	7391.8	6500	13.72	[W]
Radiators surface	31.58	28	12.79	$[m^2]$
Radiators mass	167.35	-	-	[kg]
Radiators Volume	0.6315	-	-	$[m^3]$
Heat to give to the lander	-	-	-	[W]
Heaters mass	-	-	-	[kg]

Table 15: TCS validation values

Unfortunately, TCS is the subsystem for which most of the outputs to be validated are missing. It is complicated to find such specific data in the literature. On the other hand, TCS, in general is one of the subsystems that has the least influence on the total weight of the lander.

5.7 Electrical Power System

To validate EPS design routine, the project data of [52] are used. Table 16 shows the comparison between [52] results and methodology final data of this thesis.

NUMERICAL INPUT

- Power budget of all subsystems: 2256 W
- Type of battery: Li-Ion
    - $Energy_{battery}$: 6.5 Wh
    - Battery energy density: $140\frac{Wh}{kg}$

Fuel cell

- Type: H2-O2
- Number of tanks N: 2
- Tanks material: DURAL 2024
    - Yield tension: 300 MPa
    - Density: 2700 $\frac{kg}{m^3}$

EPS	Thesis	[52]	Error [%]	Unit
EPS TOTAL MASS (FUEL CELLS)	220.54	186	18.57	[kg]
Battery capacity	99.4	78	27.43	[Ah]
Battery mass	19.88	20.7	-3.96	[kg]
H2 mass	7.78	6.2	25.48	[kg]
O2 mass	61.39	48.8	25.8	[kg]
H2 tank mass	101.47	88	15.31	[kg]

O2 tank mass	49.9	43	16.04	[kg]

Table 16: EPS validation values

Considering the batteries, except for the capacity, the mass is almost identical. As for the fuel cells, the mass of hydrogen and oxygen deviate somewhat from the values in [52] since eqs. (4.114) and (4.115) used are very simplified and consider only the power budget and average cell voltage.

Chapter 6

Conclusion and future works

This final chapter will report the conclusions of the work done and list possible improvements for future work that could use the following thesis as a starting point.

6.1 Final results discussion

Resuming what was written in *1.3 Thesis Objectives & Breakdown of Work*, the main objective of the thesis work was to lay the groundwork for the creation of a tool that implements a methodology for the design of a multifunctional manned lander that performs both descent and ascent on Mars. The study to create the tool is divided into two main blocks:

- a first block for the routine part of mission analysis;
- a second block for the routine design part of the various subsystems of the lander, work on which this thesis focused.

In Subsystem Design, through the drafting of a series of inputs to be chosen by the user, a series of outputs were obtained through sizing algorithms. The results obtained are an initial estimate of the mass and volume budgets of each subsystem and an initial estimate of the peak power required by the lander and were derived through the choice of ad hoc inputs. Regarding the estimation of the mass budget of the various subsystems and the total dry mass of the lander, the results have been reported in the paragraph *4.10 New subsystems percentages on ascent dry mass* and dry mass obtained is 17921 kg. This result is lower than that obtained by optimal staging and was derived by summing only the principal components from which each subsystem is composed.

As for the estimation of the volume budget, the main results are given in the sections on each subsystem in Subsystem Design, and again the volume of the main components of each subsystem was considered. The power budget, as already anticipated in section *4.8.2 Sizing Algorithm* was calculated by a semi-empirical formula of [25], this is because the preliminary design did

not go into such detail as to be able to estimate the power budget of each subsystem. This aspect is one of the main limitations of the following thesis.

6.2 Improvements for future works

Taking the following thesis as a starting point, the main improvements and insights to be made for possible future work are as follows:

1. Integrate the subsystems design routine with the mission analysis routine, which, as mentioned earlier, is covered in a thesis work parallel to this one. Specifically, one should pass to the mission analysis routine subsystems data mainly concerning size, masses, and, for the propulsion subsystem, propellant performance and mass, data that were obtained using an arbitrary ΔV value as input. Once this was done, the mission analysis routine, which is currently validated on a reference vehicle [20], should use the data provided to calculate the ΔV for the two scenarios and the mass of propellant consumed. If the difference between the ΔV and propellant mass entered in the mission analysis routine and the actual calculated values resulted with a percentage error less than a threshold, the final lander design and final flight path would be found.
   Figure 43 shows how tool should work.
2. Make further iterations to increase the degree of depth of design of all subsystems. The sizing that has been done in this thesis work is preliminary and high-level, so an excellent future cue may be to go into even more detail for each subsystem so that the calculation of the various mass, volume, and power budgets can be improved and made more accurate. This can be done by removing simplifying assumptions, considering more components for each subsystem, and using more complicated sizing algorithms.
3. Writing the tool that includes both complete routines on Python. This would allow a graphical interface to be presented to the user, who with input would get outputs constituting the sizing of the lander subsystems and a simulation of descent and ascent trajectory with relative parameters on Martian soil.

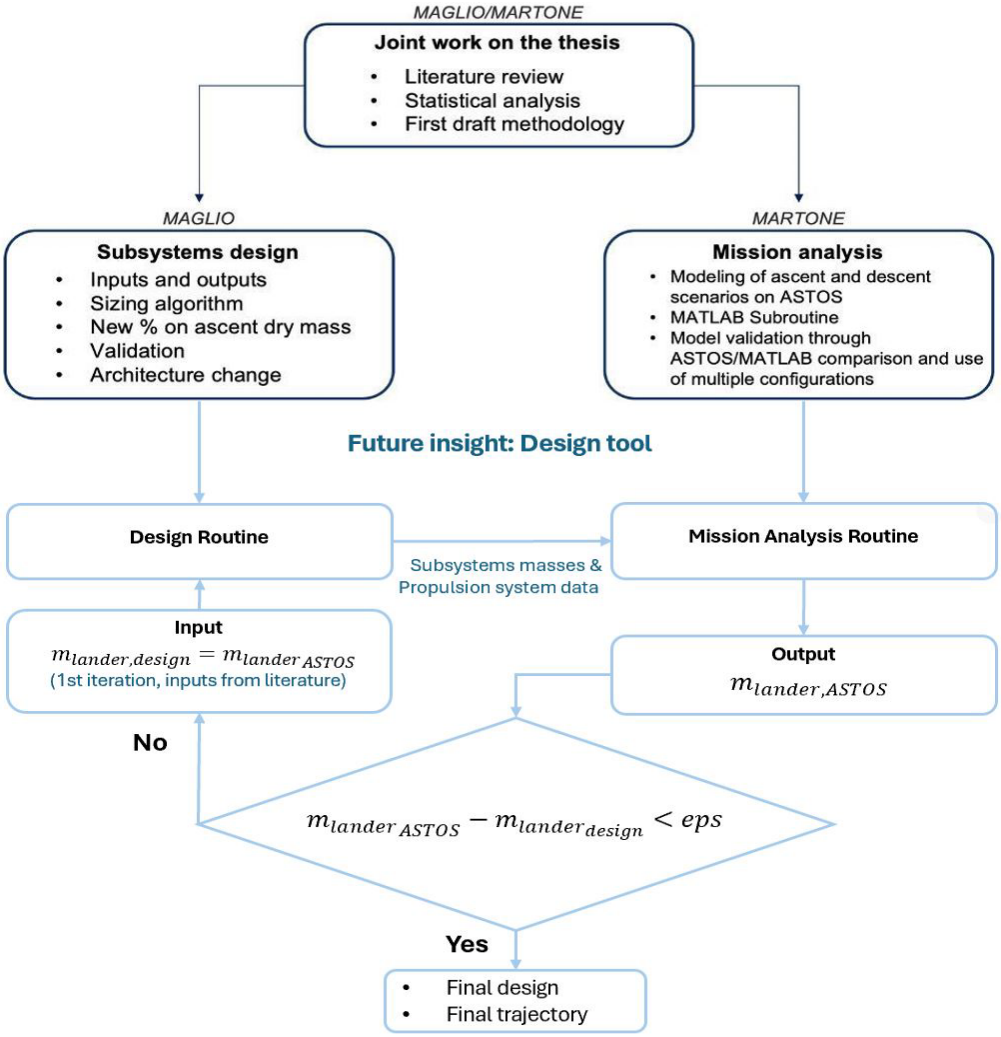

Figure 43: Future Improvements: Design Tool

Bibliography

[1] https://science.nasa.gov/mission/viking/
[2] https://science.nasa.gov/mission/mars-pathfinder/
[3] https://www.jpl.nasa.gov/missions/mars-science-laboratory-curiosity-rover-msl
[4] https://www.space.com/perseverance-rover-mars-2020-mission
[5] "Human Exploration of Mars Design Reference Architecture 5.0, Mars Architecture Steering Group, 2009".
[6] "Starship users guide", Revision 1.0 March 2020
[7] "Entry, Descent and Landing Systems Analysis: Exploration Class Simulation Overview and Results", Cianciolo D. A. et al., 2020.
[8] "High MassMars Entry, Descent, and Landing Architecture Assessment", Steinfeldt et al., 2020.
[9] "Argo Nova: Spacecraft and Mission Design of a Heavy Mars Lander", Naik et al., 2020.
[10] Design and testing of the inflatable aeroshell for the IRVE-3 flight experiment", Lichodziejewski et al., 2012.
[11] "Crewed Mars Ascent Stages: Propellant Options, Configuration, Alternatives and Performance", Benjamin Donahue, Matt Duggan. The Boeing Company, Huntsville, AL, 35758, and Houston, TX, 77058, USA.
[12] "Human Exploration of Mars Design Reference Architecture 5.0 Addendum #2", Bret G. Drake and Kevin D. Watts., Technical Report NASA/SP–2009- 566-ADD2. Houston, Texas: NASA Johnson Space Center, 2009.
[13] "From the Martian Surface to Its Low Orbit in Reusable Single-Stage Vehicle", Jérémie Gaffarel et al.
[14] "Lightweight Mars Ascent Vehicle", Alexander Seligson, Harris Paspuleti, Andrew Huh, Hannah Quirk. Faculty Adviser: Professor Sven Haverkamp. Cooper Union, April 20th, 2021
[15] "System Design Of A Mars Ascent Vehicle", by Scott Alan Geels. S. B. Aeronautics and Astronautics Massachusetts Institute of Technology (1989)
[16] "A High-Heritage Blunt-Body Entry, Descent, and Landing Concept for Human Mars Exploration", H. , R. Manning, E.

Sklyanskiy and R. Braun. Jet Propulsion Laboratory, Pasadena, California
[17] "Mars Ascent Vehicle Design for Human Exploration", Tara Polsgrove et al. NASA, George C. Marshall Space Flight Center, Huntsville, AL, 35812
[18] "A Practical Architecture for Exploration-Focused Manned Mars Missions Using Chemical Propulsion, Solar Power Generation and In-Situ Resource Utilisation", D.Willson, J.D.A Clarke
[19] "Mars Expedition – Project Hugin & Munin Transfer Vehicles Design", Maria Pilar Alliri, Mounib Bouaissa, Ludovico Bravetti, Moritz Disson, Robin Duprat, Jennifer Ly. MSc students, KTH, Royal Institute of Technology, Stockholm, Sweden
[20] "FEASIBILITY STUDY ON A CREWED MARS LANDER", Andrea Paternoster, Politecnico di Torino - Thales Alenia Space Italia - ISAE Supaero Toulouse, Italy
[21] Alicia Dwyer Cianciolo et al. "Human Mars Entry, Descent and Landing Architecture Study: Deployable Decelerators". (2019). NASA Langley Research Center, NASA Marshall Space Flight Center, NASA Ames Research Center.
[22] Tara Polsgrove et al. "Human Mars Lander Design for NASA's Evolvable Mars Campaign". Marshall Space Flight Center, Langley Research Center, Johnson Space Center, Jet Propulsion Laboratory, Goddard Space Flight Center. Huntsville, AL et al. NASA, 2016.
[23] Ashley M. Korzun et al. "A concept for the entry, descent, and landing of high-mass payloads at Mars". In: Acta Astronautica (2009). Georgia Institute of Technology, NASA Johnson Space Center, Jet Propulsion Laboratory, California Institute of Technology
[24] Tara P. Polsgrove et al. "Human Mars Entry, Descent and Landing Architecture Study: Rigid Decelerators". NASA Marshall Space Flight Center, NASA Langley Research Center, NASA Johnson Space Center, NASA Ames Research Center.
[25] Wiley J. Larson and Linda K. Pranke. "Human Space Flight: Mission Analysis and Design.", 1st. McGraw-Hill College, Oct. 1999.
[26] K. Suresh e B. Sivan, Integrated Design for Space Transportation Systems, Springer, 2015.
[27] Thesis "Performance Requirements for a Descent and an Ascent Lunar Engine", Mormile F.
[28] "Space Mission Engineering: The New SMAD", Wertz J. R., Everett D. F., Puschell J. J.
[29] M. K. Ewert, T. T. Chen, and C. D. Powell, "Life Support Baseline Values and Assumptions Document," 2022.

[30] "Living Together in Space: The Design and Operation of the Life Support Systems on the International Space Station."
[31] A. E. G. V. K. C. O. Kevin Takada, "Oxygen Generation Assembly Design for Exploration".
[32] "Historical volume estimation and a structured method for calculating habitable volume for in-space and surface habitats", Simon M., Bobskill M.R., Wilhite A.
[33] "Bounding the Spacecraft Atmosphere Design Space for Future Exploration Missions", Kevin E. Lange, Alan T. Perka, Bruce E. Duffield and Frank F. Jeng Jacobs Sverdrup ESC Group
[34] F. Castellini, Multidisciplinary Design Optimization for expendable launch vehicles, 2012.
[35] Slides *"Endoreattori"*, Prof. Pastrone
[36] Human Mars Entry, Descent and Landing Architecture Study: Deployable Decelerators Alicia Dwyer Cianciolo, Robert Dillman, Andrew Brune, Rafael Lugo NASA Langley Research Center, Hampton, VA, 23681, U.S.A
[37] Master of scienze Thesis "Develope of a Liquid Bi-Propellant Rocket Engine Design, Analysis and optimization Tool", R.R.L. Ernst
[38] "Update to Mars Ascent Vehicle Design for Human Exploration", Tara Polsgrove
[39] "Design of a Novel Hypersonic Inflatable Aerodynamic Decelerator for Mars Entry, Descent, and Landing", Li L.,Rossman G.,Skolnik N.,Kamezawa H., Longo A.
[40] "Entry, Descent and Landing Systems Analysis Study: Phase 1 Report"
[41] Slides "Communication System", Prof. Corpino
[42] Slides "Electrical Power System", Prof. Corpino
[43] "Fuel Cell Systems Explained'', Second Edition, James Larminie and Andrew Dicks
[44] https://blog.wika.us/products/pressure-products/hydrogen-vehicles-pressure-sensors-key-safety-component/
[45] https://science.nasa.gov/technology/technology-highlights/surviving-the-lunar-night-drps-could-enable-the-power-to-explore
[46] Ref: J. Zakrajsek, "RPS Program Technology Updates", Ocean Worlds and Dwarf Planets Panel of the 2023-2032 Planetary Science and Astrobiology Decadal Survey (March 2021).
[47] 2"Lunar Surface-to-Surface Power Transfer", Thomas W. Kerslake Glenn Research Center, Cleveland, Ohio.

[48] “Human Mars Entry, Descent and Landing Architecture Study: Descent Systems”, Thomas K. Percy, Tara Polsgrove, Steve Sutherlin, NASA, George C. Marshall Space Flight Center, Huntsville, AL, 35812, U.S.A.
[49] “Human Mars Mission Design Study Utilizing the Adaptive Deployable Entry and Placement Technology”, Alan M. Cassell, Chad A. Brivkalns, Jeff V. Bowles, Joseph A. Garcia, David J. Kinney, Paul F. Wercinski NASA Ames Research Center Moffett Field, CA 94035
[50] “Human Mars Entry, Descent and Landing Architecture Study: Deployable Decelerators”, Alicia Dwyer Cianciolo, Robert Dillman, Andrew Brune, Rafael Lugo NASA Langley Research Center, Hampton, VA, 23681, U.S.A
[51] “NASA Lunar Lander Reference Design”, L.D. Kennedy Marshall Space Flight Center, Huntsville, Alabama
[52] “Lunar Lander Conceptual Design”, NASA Lyndon B. Johnson Space Center Advanced Projects Office
[53] https://www.enginehistory.org/Rockets/RPE09.44/RPE09.44.shtml
[54] https://www.enginehistory.org/Rockets/RPE09.43/RPE09.43.shtml
[55] “Overview of the Altair Lunar Lander Thermal Control System Design and the Impacts of Global Access”, Ryan A. Stephan